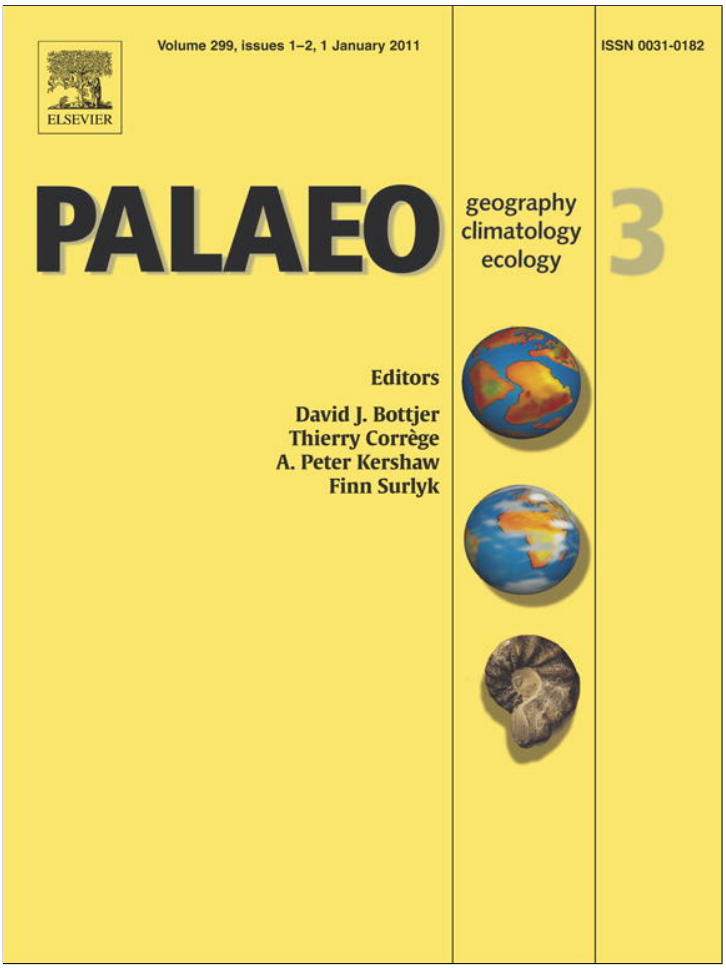

Palaeogeography, Palaeoclimatology, Palaeoecology 299 (2011) 250–264

Contents lists available at ScienceDirect

Palaeogeography, Palaeoclimatology, Palaeoecology

journal homepage: www.elsevier.com/locate/palaeo

# Reconstructing the palaeoenvironment of the Middle Russian Sea during the Middle–Late Jurassic transition using stable isotope ratios of cephalopod shells and variations in faunal assemblages

Hubert Wierzbowski [a,*], Mikhail Rogov [b]

[a] Institute of Geological Sciences, Polish Academy of Sciences, Research Centre in Warsaw, ul. Twarda 51/55, PL 00-818 Warszawa, Poland
[b] Geological Institute, Russian Academy of Sciences, Pyzhevsky lane 7, 119017 Moscow, Russia

ARTICLE INFO

*Article history:*
Received 11 February 2010
Received in revised form 6 October 2010
Accepted 4 November 2010
Available online 9 November 2010

*Keywords:*
Stable isotopes
Carbonate
Paleoclimate
Ammonite assemblages
Callovian
Oxfordian

ABSTRACT

Oxygen and carbon isotope data of well-preserved belemnite rostra and ammonite shells are presented from the Callovian–Oxfordian boundary (uppermost Lamberti to lowermost Cordatum zones) of the Dubki section near Saratov in the Russian Platform. Palaeotemperatures calculated for nektobenthic belemnites (averages of 5 °C and 8 °C for cylindroteuthids and belemnopseids, respectively) show the presence of cold bottom waters in the central part of the Middle Russian Sea during the studied interval. Palaeotemperatures calculated for ammonites, which are assumed to have lived in near-surface waters, are considerably higher (average 13 °C). The presented data show a vertical thermal gradient in the Middle Russian Sea. The belemnite oxygen isotope record and the relative abundances of ammonite families in the Dubki section do not correlate with each other probably as a result of different depth habitats of ammonites and belemnites. A review of literature isotope data shows the climatic zonation in European seas at the Middle–Late Jurassic transition. Despite the flux of cold polar waters to the Middle Russian Sea and the area of Scotland there is no evidence for glaciation at the Middle–Late Jurassic transition. Changes in water circulation during a sea-level highstand were likely a source of spreads of cold bottom waters and cardioceratid ammonite fauna in this time period.

The belemnite isotope record of the Callovian–Oxfordian boundary in the Russian Platform is characterized by significant scatter of $\delta^{13}C$ values. No temporal carbon isotope trend is observed. The $\delta^{13}C$ values of Russian belemnite rostra average 2.6‰ VPDB being 1 to 2‰ higher than the values of coeval Lower Oxfordian belemnites from the area of the Submediterranean ammonite province. Higher (than Submediterranean) $\delta^{13}C$ values of Russian belemnite rostra are likely related to high biologic productivity and/or high organic matter burial in semi-isolated Boreal–Subboreal marine basins.



## 1. Introduction

Oxygen isotope records of belemnite rostra and fish teeth from the Russian Platform, eastern France and western Switzerland show prominent decreases in seawater temperature during the Late Callovian–Early Oxfordian (Barskov and Kiyashko, 2000; Dromart et al., 2003a,b; Lécuyer et al., 2003; Podlaha et al., 1998; Price and Rogov, 2009; Riboulleau et al., 1998; Veizer et al., 1999). Relatively constant seawater temperatures during the Callovian and the Oxfordian accompanied by strong perturbations in the global carbon cycle are on the other hand reported from central Poland (Wierzbowski, 2002; Wierzbowski et al., 2009). There is no agreement on a scale and a source of the observed isotope variations at the Middle–Late Jurassic transition. Dromart et al. (2003a,b) and Lécuyer et al. (2003) suggested the occurrence of abrupt climatic changes i.e. a Middle Callovian thermal optimum, an ice age in the Late Callovian–Early Oxfordian, and a global warming starting from the Middle Oxfordian. The interpretation of Dromart et al. (2003a,b) and mass balance models of Louis-Schmid et al. (2007) additionally assumed low atmospheric $pCO_2$ level as distinctive of a cool Late Callovian–Early Oxfordian period. According to the interpretation of Wierzbowski et al. (2009) a prominent Late Callovian sea-level rise may have led to the $\delta^{13}C_{carbonate}$ excursion, changes in water circulation and have constituted an important factor of faunal migrations. The isotope record of the Russian Platform which is characterized by an abrupt increase of 7–16 °C in the calculated seawater temperature during the Oxfordian (cf. Price and Rogov, 2009) is exceptional and was differently interpreted by Dromart et al. (2003a, b) and Wierzbowski et al. (2009).

This study is based on calcareous fossils from the Upper Callovian–Lower Oxfordian (uppermost Lamberti to lowermost Cordatum zones) of the Russian Platform. The focus of this contribution is to determine the isotope composition of different groups of fossils: belemnopseid and cylindroteuthid belemnites, which are considered to have been nektobenthic dwellers, and

* Corresponding author. Fax: +48 22 620 62 23.
*E-mail address:* hwierzbo@twarda.pan.pl (H. Wierzbowski).

0031-0182/$ – see front matter © 2010 Elsevier B.V. All rights reserved.
doi:10.1016/j.palaeo.2010.11.006

ammonites, which are interpreted to have lived in shallower waters (cf. Anderson et al., 1994; Lécuyer and Bucher, 2006; Lukeneder et al., 2010; Price and Page, 2008; Wierzbowski, 2002; Wierzbowski and Joachimski, 2007). This methodology is used to obtain a multi-element dataset for the reconstruction of palaeoenvironment. The present study also provides discussion on possible sources of the distribution of ammonite and belemnite faunas. This approach is intended to shed light on the isotope record of the Russian Platform and expand knowledge of the Jurassic climate and oceanography.

## 2. Geologic setting

The Dubki section is located ~5 km NNE of Saratov (Fig. 1). Studied sediments were deposited in the Volga Basin — a central part of the epicontinental Middle Russian Sea connected with the Arctic Sea and the Tethys (Fig. 2). The Saratov area was situated at a palaeolatitude of 40–45°N during the Late Callovian and the Early Oxfordian (Fig. 2). Upper Callovian and Lower Oxfordian sediments exposed in Dubki have a thickness of 8.85 m and consist of dark and calcareous clays with phosphorite and pyrite concretions (Fig. 3). The sediments are rich in well-preserved fossils (bivalves, belemnites, ammonites, gastropods, bryozoans, decapods and ostracods; cf. Tesakova, 2008). Strongly calcareous clay and a 0.35 m thick marly layer occur in the uppermost part of the section (Fig. 3).

The sediments were deposited below storm weather wave as shown by the absence of storm deposits and the presence of a very low-energy environment. A significant depth of the basin is also shown by a diversified ostracod assemblage typical of the sublitoral zone (Tesakova, 2008). The presence of a rich and differentiated benthic fauna indicates well-oxygenated bottom conditions. The rich cephalopod and bryozoan fauna as well as findings of brachiopods and crinoids in Dubki point to normal marine salinity of the Middle Russian Sea in the Saratov area during the Callovian–Oxfordian transition. The long distance from land areas and the absence of freshwater flux to the basin may be shown by the scarcity of land plant debris in Dubki deposits (E. Tesakova and M. Ustinova; personal communication). Interestingly, the uppermost Callovian and lowermost Oxfordian in the Moscow area of the Russian Platform is also marked by the dominance of marine palynoflora in the microphytofossil assemblage (Smirnova et al., 1999). The reduction in the abundance and sharp changes in the diversity of ostracods observed in the upper part of the Mariae Zone and the Cordatum Zone in Dubki are however interpreted to have resulted from shallowing of the basin and the penetration of the sea-bottom by warm superficial currents (Tesakova, 2008).

The Dubki section is dated to the Lamberti Zone of the Callovian as well as the Mariae Zone and the lower part of the Cordatum Zone of the Oxfordian (Fig. 3). Its stratigraphy is based on ammonite fauna with employed NW European zones and subzones and local ammonite horizons (Kiselev and Rogov, 2005; Kiselev et al., 2006). Partly different ammonite horizons were previously distinguished by Mitta (2003), Keupp and Mitta (2004) as well as Rogov and Egorov (2003), who focused on the oppeliid assemblage of the uppermost section part. The lower part of the Dubki section (including the Henrici Subzone and a lowermost part of the Lamberti Subzone of the Lamberti Zone) was not exposed during sample collection.

## 3. Palaeobiogeography

The provincialism of Jurassic ammonite and belemnite fauna in Europe resulted in the development of two major biochores: the Boreal (Arctic) and the Mediterranean (Tethyan) Realm. Transitory faunistic zones like the ammonite–belemnite Boreal–Atlantic Subrealm (or Province) and ammonite Subboreal and Submediterranean provinces are also apparent in Europe (Doyle, 1987; Page, 2008; Page et al., 2009; Stevens, 1973; Westermann, 2000). The central part of the Middle Russian Sea — the Volga Basin was predominantly settled by Boreal–Subboreal ammonites (cardioceratids and kosmoceratids) in the course of the Late Callovian and the Early Oxfordian. Other ammonites (aspidoceratids, perisphinctids and oppeliids) that usually inhabited Submediterranean and Mediterranean provinces were also present in this area as result of a marked fauna overlap observed in Europe at the Callovian–Oxfordian transition (cf. Matyja and Wierzbowski, 1995). The mixed faunal assemblage of the Middle Russian Sea is typical of the ammonite Subboreal Province (*sensu* Page et al., 2009). The Saratov area of the Middle Russian Sea was settled by Boreal (cylindroteuthid) and Tethyan (belemnopseid) belemnites. The belemnopseid belemnite rostra (genus *Hibolithes*) are numerous in the Dubki section but small

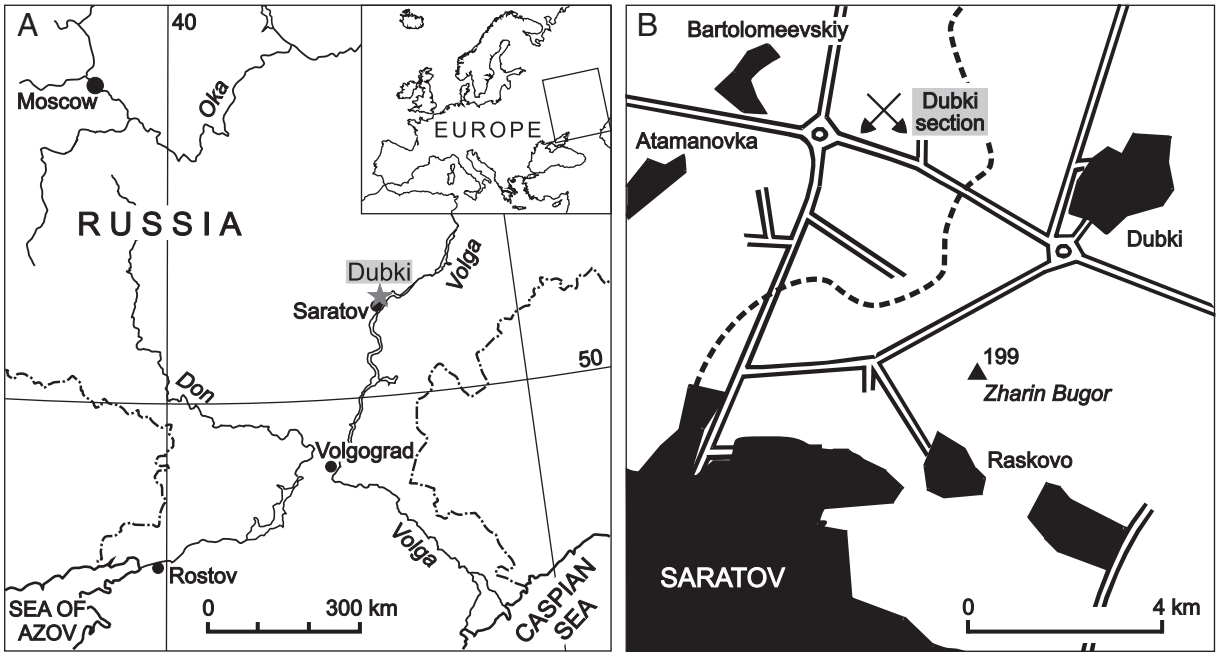


**Fig. 1.** A — Location of Dubki near Saratov in Russia, B — Location of the Dubki outcrop.

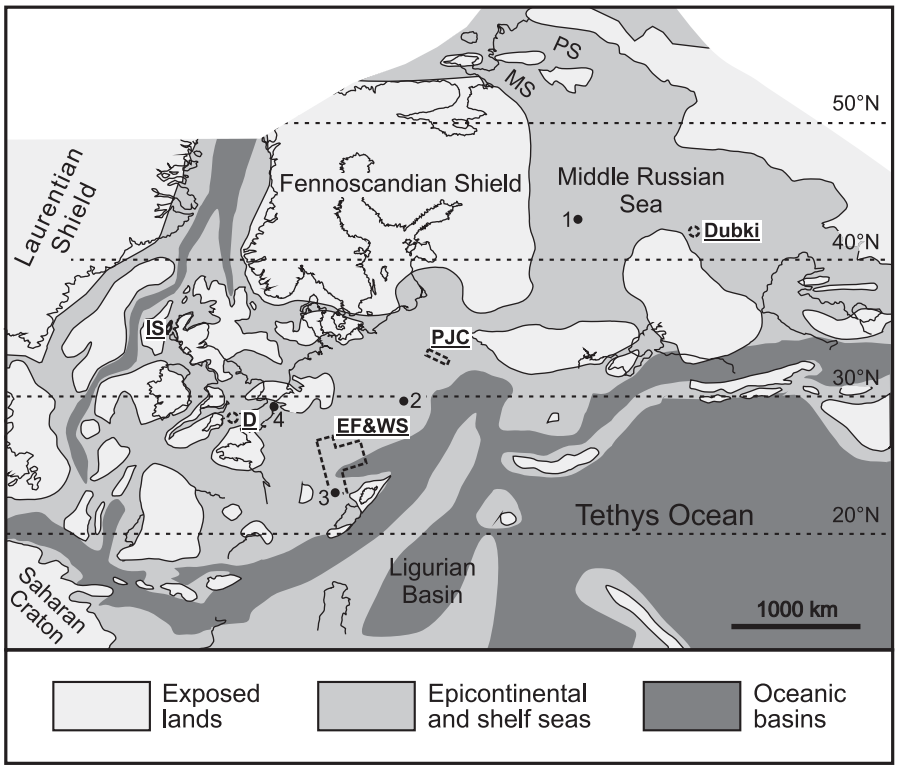


**Fig. 2.** Palaeogeography of the Early Oxfordian in Europe (after Ziegler, 1990 and Thierry et al., 2000a,b; modified according to the data of Gaździcka, 1998; Golonka, 2004; Sazonova and Sazonov, 1967; Świdrowska et al., 2008). MS — Mezen strait. PS — Pechora strait. Areas of isotope studies (referred in Sections 7.1. and 7.3.): D — Dorset, EF&WS — eastern France and western Switzerland, IS — Isle of Skye, PJC — Polish Jura Chain. Localities studied for variations in ammonite assemblage (referred in Section 7.2.): 1 — Mikhailov, Russia, 2 — Sengenthal, Germany, 3 — SE Basin, France, 4 — Uzelot, France.

(maximal length below 5 cm). The mixed-assemblage of Boreal cylindroteuthids and Mediterranean belemnopseids is characteristic of the belemnite Boreal–Atlantic Province (cf. Doyle, 1987).

The distribution of Middle–Late Jurassic marine fauna in Europe was given as an evidence for climatic zonation, environmental stability and the existence of physical barriers and sea currents (cf. Fürsich and Sykes, 1977; Ziegler, 1965). There is also no consensus about a source of variations in the ammonite assemblage at the Callovian–Oxfordian transition i.e. the spread of Boreal ammonites and the marked ammonite fauna overlap were given as evidences for global glaciation (Dromart et al., 2003a,b) or a global sea-level rise (Matyja and Wierzbowski, 1995; Wierzbowski et al., 2009).

## 4. Materials and methods

The sediments yielded ammonites, belemnites and bivalves. The collected ammonites are represented by *Quenstedtoceras*, *Cardioceras* and *Vertumniceras* (family Cardioceratidae), *Euaspidoceras* and *Peltoceras* (family Aspidoceratidae), *Sublunuloceras* (family Oppeliidae). The belemnites belong to the genera: *Hibolithes* (family Belemnopseidae), *Cylindroteuthis* and *Lagonibelus* (family Cylindroteuthidae). The studied bivalves are represented by *Gryphaea* (family Gryphaeidae) and *Trigonia* (family Trigoniidae).

Thin sections prepared from calcitic belemnite rostra and bivalve shells were studied by means of cathodoluminescence microscopy. Non-luminescent fossils were subsequently cleaned with a micro-drill to remove adherent sediment, apical line infillings of the rostra and, if necessary, external, luminescent rims. Whole-dimensional fragments of belemnite rostra were powdered and homogenized in order to get average isotope values. Aliquots of the carbonate powders were used for the trace element and the isotope analysis. Trace element contents (Ca, Mg, Sr, Mn, Fe) were determined using a Perkin-Elmer Optima 5300 DV ICP-OES spectrometer after dissolving the carbonate powders in 5% hydrochloric acid. Overall reproducibility of ICP-OES analyses (1σ) was checked by replicate analysis (n = 31) of sample R144b and was better than ±0.41‰ for Ca, ±14 ppm for Mg, ± 23 ppm for Sr, ±2 ppm for Fe and ±3 ppm for Mn.

Powdered and homogenized parts of aragonitic shells (including fragments of external walls of adult portions of ammonite shells and fragments of trigoniid shells) were screened for a potential contribution of diagenetic calcite using X-ray diffraction method. 1–2 subsamples taken from each specimen were studied. Powdered samples were scanned from 28° to 63° 2Θ using D8 Advance Bruker AXS diffractometer with $CoK_\alpha$ radiation and Fe filter. X-ray diffractograms were examined for the strongest reflections of the calcite and aragonite phases. Quantitative estimation of the mineral phases was performed by Rietveld analysis using the Topas software. The preservation state of the original microstructure of pure aragonitic (>99%) shells was examined with a scanning electron microscope (SEM).

Carbonate samples were reacted with 100% $H_3PO_4$ at 70 °C in an online, automated carbonate reaction device (Kiel IV) connected to a Finnigan Mat Delta Plus mass spectrometer at the Institute of Geological Sciences and the Institute of Palaeobiology, Polish Academy of Sciences in Warsaw. Isotopic ratios were referenced to NBS19 international standard ($\delta^{13}C = 1.95‰$, $\delta^{18}O = -2.20‰$). The oxygen isotope composition of aragonite was calculated from the $\delta^{18}O$ value of evolved $CO_2$ using the acid fractionation factor of 1.00883, which is the estimated value of the conventional acid fractionation factor for aragonite at 70 °C (conventional $\alpha_{CO2\text{-}aragonite}$ amounts to 1.01034 at 25 °C; see Friedman and O'Neil, 1977. Its estimated value for 70 °C was calculated using the temperature dependence of the factor given by Kim et al., 2007 although the absolute, revised values of the factor reported by Kim et al., 2007 differ from conventional ones). All oxygen and carbon isotope results are reported in δ notation in per mil relative to the VPDB international standard. Reproducibility (1σ) of isotope measurements was checked by replicate analysis

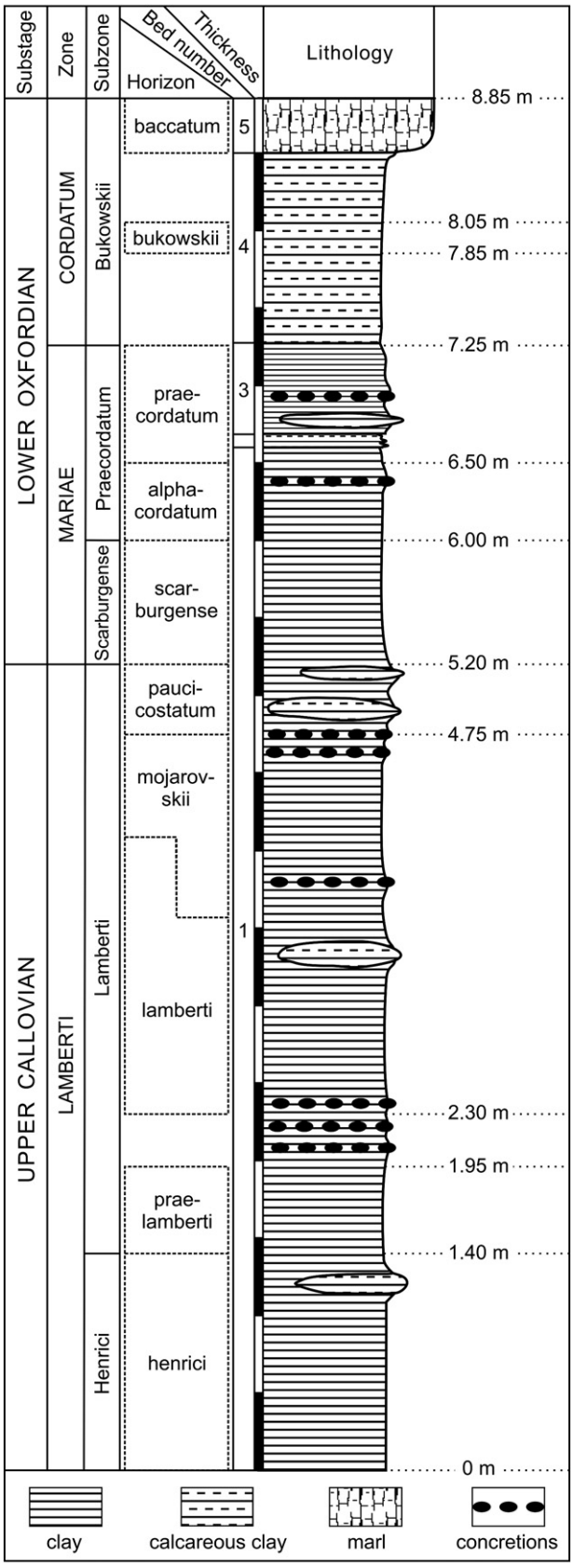


**Fig. 3.** Lithology and stratigraphy of the Dubki section. Biostratigraphy based on Kiselev et al. (2006).

(n = 30) of laboratory reference and was better than ±0.03‰ for $\delta^{13}C$ and ±0.06‰ for $\delta^{18}O$. Palaeotemperatures were calculated from the oxygen isotope composition of calcitic belemnite rostra using the Eq. (1) of O'Neil et al. (1969) modified by Friedman and O'Neil (1977) and SMOW to PDB scales conversion given by Friedman and O'Neil (1977).

$$10^3\ ln\alpha_{calcite-water} = 2.78*10^6/T^2 - 2.89 \quad (1)$$

where $\alpha_{calcite-water}$ is equilibrium fractionation factor between calcite and water, T is the temperature in Kelvin. Temperatures calculated for the measured range of $\delta^{18}O$ values using the equation of O'Neil et al. (1969) modified by Friedman and O'Neil (1977) are 0.4 to 1.3 °C lower than the temperatures calculated using the equation of Epstein et al. (1953) corrected by Craig (1965) and modified by Anderson and Arthur (1983). The latter equation, albeit frequently used for skeletal calcite, is based on aragonite-calcitic mollusc shells (see Epstein et al., 1953) and therefore was not employed in the present study. Palaeotemperatures from aragonite fossils were calculated using the corrected version (2) of the equation of Grossman and Ku (1986) established for "mollusks". The equation of Grossman and Ku (1986) had to be standardized to the SMOW scale as the original $\delta^{18}O$ values of ambient water were reported vs. "average marine water" being 0.2‰ depleted in $^{18}O$ in comparison to the SMOW (cf. Grossman and Ku, 1986).

$$T(℃) = 21.8 - 4.69*\left(\delta^{18}O_{aragonite} - \left(\delta^{18}O_{water} - 0.2\right)\right) \quad (2)$$

where $\delta^{18}O_{aragonite}$ is the isotope composition of shell aragonite vs. PDB and $\delta^{18}O_{water}$ is the isotope composition of ambient water vs. SMOW. Precision of calculated temperatures (2σ) as resulted from the propagation of the error of oxygen isotope analyses is close to ± 0.5 °C.

## 5. Diagenetic alteration

Cementation and re-crystallization processes may alter the isotope composition of calcareous fossils. The assessment of the degree of diagenetic alteration of calcitic belemnite rostra and *Gryphaea* shells can be made using trace element concentrations. Diagenetic alteration often causes an increase in Fe and Mn concentrations in calcite as these elements become soluble under reducing conditions. Conversely, Sr contents in marine calcites decrease during diagenesis as Sr concentrations are relatively high in seawater and low in majority of diagenetic fluids (Marshall, 1992; Veizer, 1974, 1983). $Mn^{2+}$ is also found to be a main activator of orange-red cathodoluminescence which is distinctive of diagenetically altered calcites (Marshall, 1992; Savard et al., 1995).

All *Gryphaea* shells were not further investigated as they showed dull to intensive orange-red luminescence (Fig. 4A) with broad spectral emission peaks from 560 to 645 nm that are considered to be activated by $Mn^{2+}$ ions (Boggs and Krinsley, 2006). Belemnite rostra were largely non-luminescent, albeit some degree of luminescence was often found at rostrum rims and in apical line areas (Fig. 4B,C). The small luminescence parts of the rostra were removed during sample preparation. Most of the non-luminescent rostra show low Fe (<150) and Mn (<100 ppm) concentrations that characterize well-preserved samples (Table 1), (cf. Price and Rogov, 2009). The $\delta^{18}O$ and $\delta^{13}C$ values of two samples (R43, R123) showing elevated Fe and Mn contents were eliminated from the dataset. The Sr concentrations in the non-luminescent belemnite rostra range from 790 ppm to 1050 ppm for cylindroteuthids and from 1000 ppm to 1370 ppm for belemnopseids (Table 1). Although it is generally assumed that critical threshold level of Sr concentrations for pristine belemnite rostra is 900 to 950 ppm (Rosales et al., 2001, 2004) the published data are derived from Tethyan belemnites. It is possible that Boreal cylindroteuthid species, which inhabited Russian Platform, were characterized by different metabolic fractionation and had lower primary Sr contents than Tethyan belemnites such as belemnopseids. In addition, Veizer (1974) reported Sr concentrations of 800 and 1600 ppm in well-preserved belemnite

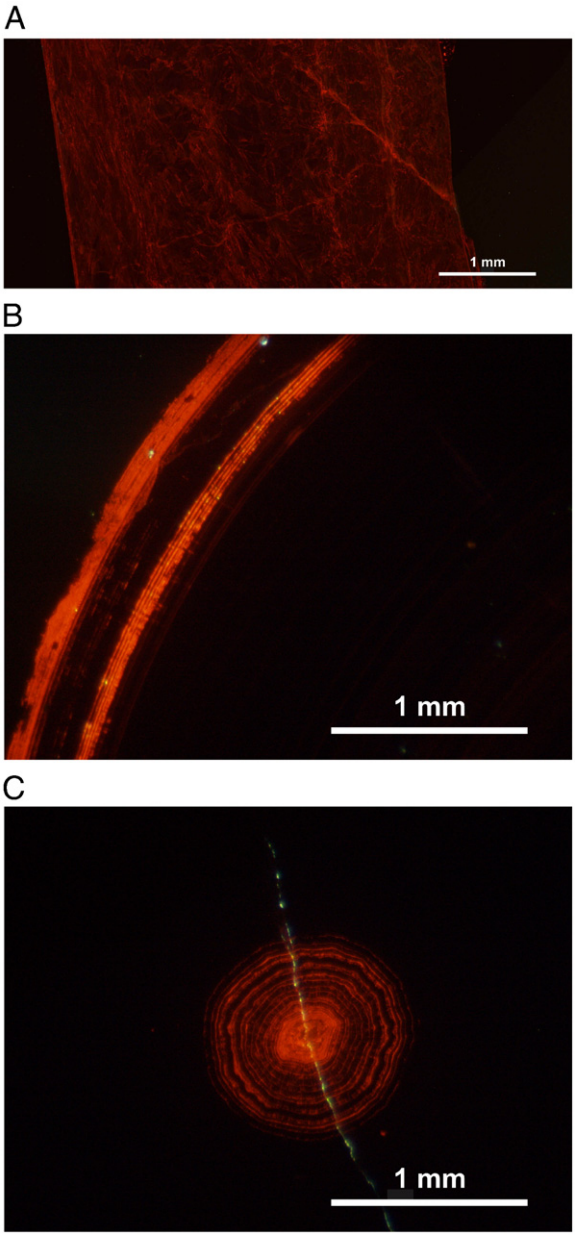


**Fig. 4.** Cathodoluminescence photomicrographs (A) Luminescent *Gryphaea* shell. Boundary of Lamberti and Mariae zones. (B) Non-luminescent *Hibolithes* rostrum with luminescent rostrum rim. Sample R120, Cordatum Zone. (C) Non-luminescent *Hibolithes* rostrum with luminescent apical line area. Sample R128, Mariae Zone.

rostra. We therefore assume the threshold level of 800 ppm as distinctive of well-preserved specimens. The $\delta^{18}O$ and $\delta^{13}C$ values of one sample (R131) showing lower Sr contents were eliminated from the dataset.

The preservation of metastable aragonite is uncommon within Jurassic deposits and it is often assumed that pure aragonitic fossils are well-preserved. Diagenetic alteration of the microstructure of aragonitic ammonite and bivalve shells was, however, observed (Buchardt and Weiner, 1981; Dauphin and Denis, 1990, 1999; Wierzbowski and Joachimski, 2007). All ammonoid and trigoniid samples that contained minor traces of calcite (>1%), as indicated by X-ray analysis, were excluded from further investigations. SEM observations allowed the identification of diagenetic alteration in the nacreous layer of adult portions of some ammonite shells and trigoniid shells despite their pure aragonite mineralogy. Dissolution and cementation of the nacreous tablets of many ammonite and all studied *Trigonia* shells were observed (Table 2, Fig. 5A,B,C). The state of preservation of the nacreous layer often was variable in different parts of the same shell. The ammonite prismatic layer was generally well-preserved. Samples characterized by total or partial alteration of the microstructure were excluded from palaeoenvironmental studies.

Interestingly, aragonitic ammonite samples with altered microstructures show a significant scatter of $\delta^{18}O$ values (−1.7 to +1.5‰; Fig. 6). Samples revealing no evidence of the alteration show in contrast a much narrower range of $\delta^{18}O$ values (−0.1 to +1.3‰; Fig. 6). A negative correlation ($r = 0.43$) significant at the 5% level between $\delta^{18}O$ values and $\delta^{13}C$ values of the altered ammonite samples is observed. We argue as a consequence that the preservation of the primary aragonitic mineralogy is not sufficient to characterize the shells as well-preserved. This is consistent with conclusion of Wierzbowski and Joachimski (2007) and implies that ammonite isotope data presented without detailed information on the microstructure preservation should be treated with caution.

## 6. Results

### 6.1. Oxygen and carbon isotopes

The $\delta^{18}O$ values of cylindroteuthid rostra (*Cylindroteuthis* and *Lagonibelus*) vary from +0.6 to +2.4‰ (average 1.7‰, Table 1, Fig. 7). The $\delta^{18}O$ values of belemnopseid rostra (*Hibolithes*) vary from +0.2 to +1.2‰ (average 0.9‰, Table 1, Fig. 7). The average $\delta^{18}O$ value of cylindroteuthids is higher by about 0.8‰ than the value of belemnopseids. Both groups of belemnites are patchily distributed across the studied section. Cylindroteuthids are present in the lower section part and disappear completely starting from the upper part of the Praecordatum Subzone of the Mariae Zone. One of two layers with abundant cylindroteuthid rostra comprising the middle part of the Praecordatum Subzone of the Mariae Zone is in turn characterized by the scarcity of belemnopseids. Observed temporal variations in the $\delta^{18}O$ values of belemnite rostra are as a result predominantly connected with changing abundances of both belemnite groups.

The cylindroteuthid $\delta^{13}C$ values oscillate between +1.5‰ and +3.8‰ (average 2.6‰; Table 1, Fig. 8). The belemnopseid $\delta^{13}C$ values oscillate between +1.7‰ and +3.4‰ (average 2.6‰, Fig. 8). The belemnite $\delta^{13}C$ values from the entire study interval show a significant scatter. No temporal trend is visible in the belemnite $\delta^{13}C$ values. The belemnite $\delta^{18}O$ and $\delta^{13}C$ values are not correlated (Fig. 9).

The $\delta^{18}O$ and the $\delta^{13}C$ values of well-preserved ammonite shells, which only occur in the lower section part, range from −0.1 to +1.3‰ (average +0.7‰) and +1.4 to +4.9‰ (average +3‰), respectively (Figs. 6–8, and Table 2). The cardioceratid ammonites (genera: *Quenstedtoceras*, *Cardioceras* and *Vertumniceras*) show higher $\delta^{18}O$ values (between +0.3 and +1.3‰, average 0.8‰) and higher and more scattered $\delta^{13}C$ values (between +2.0 and +4.9‰, average 3.4‰) compared to the $\delta^{18}O$ values (−0.1 and +0.9‰, average 0.3‰) and $\delta^{13}C$ values (+1.4 and +2.8‰, average 2.2‰) of oppeliid ammonites (genus *Sublunuloceras*). No correlation between the $\delta^{18}O$ and the $\delta^{13}C$ values of the well-preserved ammonite shells is observed (Fig. 6).

### 6.2. Mg/Ca and Sr/Ca ratios

Mg/Ca ratios of belemnite rostra vary between 4.2 and 20.4 mmol/mol (Fig. 10). Sr/Ca ratios of belemnite rostra vary between 1.0 and 1.7 mmol/mol (Fig. 11). Belemnopseid rostra show higher Mg/Ca (8.9 to 20.4) and Sr/Ca ratios (1.2 to 1.7) than cylindroteuthid rostra (4.2 to 9.6 and 1.0 to 1.2, respectively). Mg/Ca and Sr/Ca ratios of both groups of belemnites do not correlate with their $\delta^{18}O$ values (Figs. 10, 11).

**Table 1**
Age, taxonomy, chemical composition and isotope ratios of belemnite rostra. Isotope ratios in ‰ relative to VPDB.

| Sample No | Position (m) | Subzone | Taxonomy | Ca (%) | Mg (ppm) | Sr (ppm) | Fe (ppm) | Mn (ppm) | $\delta^{18}O$ (‰) | $\delta^{13}C$ (‰) |
|---|---|---|---|---|---|---|---|---|---|---|
| R43 | 8.75 | Bukowskii | *Hibolithes* sp. | 37.99 | 4501 | 1039 | 150 | 468 | – | – |
| R109 | 8.6 | Bukowskii | *Hibolithes* sp. | 37.87 | 3937 | 1371 | 64 | 135 | 0.81 | 2.12 |
| R123 | 8.6 | Bukowskii | *Hibolithes* sp. | 37.61 | 4346 | 1241 | 83 | 367 | – | – |
| R79 | 7.9 | Bukowskii | *Hibolithes* sp. | 38.91 | 3527 | 1122 | 12 | 30 | 0.83 | 2.35 |
| R45a | 7.8 | Bukowskii | *Hibolithes* sp. | 37.88 | 3028 | 1109 | 5 | 31 | 0.96 | 3.08 |
| R45b | 7.8 | Bukowskii | *Hibolithes* sp. | 38.64 | 3401 | 1088 | 5 | 4 | 0.72 | 2.43 |
| R120 | 7.8 | Bukowskii | *Hibolithes* sp. | 38.28 | 4245 | 1147 | 7 | 3 | 1.05 | 2.8 |
| R65 | 7.7 | Bukowskii | *Hibolithes* sp. | 39.11 | 4305 | 1296 | 5 | 10 | 1.17 | 2.63 |
| R84 | 7.45 | Bukowskii | *Hibolithes* sp. | 37.68 | 4412 | 1249 | 5 | 6 | 0.9 | 2.82 |
| R96 | 6.9 | Praecordatum | *Hibolithes* sp. | 38.62 | 3936 | 1201 | 6 | 1 | 0.96 | 2.32 |
| R89 | 6.75 | Praecordatum | *Cylindroteuthis* sp. | 38.78 | 1396 | 820 | 2 | 7 | 2.13 | 2.8 |
| R124 | 6.75 | Praecordatum | *Cylindroteuthis* sp. | 39.09 | 1231 | 849 | 2 | 5 | 1.62 | 1.86 |
| R134a | 6.6 | Praecordatum | *Cylindroteuthis* sp. | 39.71 | 1197 | 972 | 4 | 17 | 1.63 | 2.95 |
| R134b | 6.6 | Praecordatum | *Cylindroteuthis* sp. | 39.27 | 1571 | 914 | 5 | 14 | 2.03 | 3.76 |
| R144b | 6.55 | Praecordatum | *Cylindroteuthis* sp. | 38.43 | 1725 | 944 | 2 | 1 | 1.67 | 1.92 |
| R 147 | 6.55 | Praecordatum | *Cylindroteuthis* sp. | 40.04 | 1235 | 1046 | 3 | 32 | 2.01 | 3.38 |
| R 157 | 6.55 | Praecordatum | *Cylindroteuthis* sp. | 37.74 | 1019 | 914 | 1 | 0 | 1.88 | 2.91 |
| R116 | 6.15 | Praecordatum | *Cylindroteuthis* sp. | 38.49 | 2050 | 823 | 2 | 5 | 1.8 | 1.9 |
| R125 | 6.15 | Praecordatum | *Hibolithes* sp. | 38.73 | 2678 | 1028 | 3 | 10 | 0.94 | 2.69 |
| R162 | 6.1 | Praecordatum | *Cylindoteuthis* sp. | 38.88 | 1206 | 846 | 3 | 8 | 1.39 | 1.87 |
| R172 | 6.1 | Praecordatum | *Cylindroteuthis* sp. | 40.66 | 2376 | 898 | 2 | 17 | 1.1 | 1.94 |
| R91 | 5.95 | Scarburgense | *Hibolithes* sp. | 38.28 | 3006 | 1138 | 3 | 12 | 1.02 | 2.65 |
| R130 | 5.85 | Scarburgense | *Hibolithes* sp. | 38.58 | 2255 | 1006 | 1 | 7 | 0.84 | 3.39 |
| R142a | 5.85 | Scarburgense | *Hibolithes* sp. | 39.59 | 3041 | 1207 | 4 | 3 | 0.22 | 2.71 |
| R142b | 5.85 | Scarburgense | *Hibolithes* sp. | 38.08 | 3742 | 1177 | 6 | 11 | 0.84 | 3.15 |
| R142c | 5.85 | Scarburgense | *Hibolithes* sp. | 39.17 | 3277 | 1103 | 2 | 5 | 0.73 | 2.18 |
| R143 | 5.85 | Scarburgense | *Hibolithes* sp. | 39.37 | 2217 | 1065 | 2 | 3 | 1.14 | 3.08 |
| R160 | 5.8 | Scarburgense | *Lagonibelus* sp. | 39.43 | 1019 | 932 | 1 | 3 | 1.74 | 3.07 |
| R136 | 5.65 | Scarburgense | *Hibolithes* sp. | 39.16 | 2565 | 1084 | 5 | 37 | 0.94 | 2.44 |
| R159 | 5.65 | Scarburgense | *Hibolithes* sp. | 39.74 | 2574 | 1065 | 1 | 15 | 0.98 | 2.59 |
| R131 | 5.55 | Scarburgense | *Lagonibelus* sp. | 39.27 | 1548 | 794 | 4 | 6 | – | – |
| R128 | 5.55 | Scarburgense | *Hibolithes* sp. | 38.72 | 2776 | 1020 | 1 | 12 | 0.88 | 2.44 |
| R 42 | 5.5 | Scarburgense | *Cylindroteuthis* sp. | 38.92 | 1001 | 875 | 3 | 12 | 1.53 | 2.55 |
| R90 | 5.6 | Scarburgense | *Hibolithes* sp. | 39.49 | 2327 | 1061 | 1 | 3 | 0.76 | 2.75 |
| R135 | 5.5 | Scarburgense | *Hibolithes* sp. | 39.01 | 3231 | 1155 | 3 | 3 | 0.83 | 2.75 |
| R137a | 5.4 | Scarburgense | *Hibolithes* sp. | 38.13 | 4707 | 1230 | 4 | 6 | 0.89 | 2.06 |
| R137b | 5.4 | Scarburgense | *Hibolithes* sp. | 37.85 | 4072 | 1216 | 5 | 5 | 1 | 2.82 |
| R60 | 5.25 | Scarburgense | *Hibolithes* sp. | 40.11 | 2171 | 1100 | 3 | 16 | 1.12 | 2.73 |
| R86a | 5.25 | Scarburgense | *Cylindroteuthis* sp. | 39.39 | 1183 | 901 | 2 | 2 | 1.85 | 2.9 |
| R86b | 5.25 | Scarburgense | *Cylindroteuthis* sp. | 39.08 | 1446 | 998 | 4 | 2 | 1.8 | 3.73 |
| R92a | 5.25 | Scarburgense | *Cylindroteuthis* sp. | 40.05 | 1521 | 973 | 2 | 11 | 1.64 | 2.57 |
| R92b | 5.25 | Scarburgense | *Cylindroteuthis* sp. | 39.21 | 1383 | 942 | 2 | 2 | 0.61 | 2.54 |
| R92c | 5.25 | Scarburgense | *Cylindroteuthis* sp. | 39.10 | 1661 | 900 | 2 | 4 | 2.02 | 2.27 |
| R98 | 5.2 | Lamberti/Scarburgense | *Lagonibelus* sp. | 39.19 | 1265 | 919 | 4 | 13 | 1.56 | 3.46 |
| R151 | 5.2 | Lamberti/Scarburgense | *Lagonibelus* sp. | 39.27 | 1284 | 913 | 4 | 13 | 1.76 | 3.16 |
| R53b | 5.2 | Lamberti/Scarburgense | *Hibolithes* sp. | 39.52 | 2537 | 1047 | 6 | 10 | 0.99 | 2.86 |
| R149 | 5.15 | Lamberti | *Cylindroteuthis* sp. | 39.03 | 2083 | 891 | 2 | 24 | 1.72 | 1.51 |
| R155 | 5.15 | Lamberti | *Cylindroteuthis* sp. | 40.08 | 1162 | 904 | 5 | 31 | 1.76 | 2.13 |
| R 37 | 5.1 | Lamberti | *Cylindroteuthis* sp. | 39.03 | 1568 | 869 | 2 | 4 | 1.71 | 1.82 |
| R113 | 5.1 | Lamberti | *Lagonibelus* sp. | 38.91 | 1212 | 886 | 2 | 7 | 1.85 | 3.41 |
| R153 | 5.1 | Lamberti | *Hibolithes* sp. | 39.55 | 3644 | 1248 | 3 | 7 | 0.89 | 2.88 |
| R56 | 4.75 | Lamberti | *Hibolithes* sp. | 39.63 | 2703 | 1048 | 2 | 16 | 1.12 | 2.05 |
| R77a | 4.75 | Lamberti | *Hibolithes* sp. | 37.52 | 3058 | 1102 | 2 | 2 | 0.9 | 2.73 |
| R77b | 4.75 | Lamberti | *Hibolithes* sp. | 40.09 | 2364 | 1104 | 3 | 57 | 1.12 | 2.6 |
| R39 | 4.65 | Lamberti | *Lagonibelus* sp. | 39.30 | 1122 | 922 | 2 | 3 | 2.35 | 3.15 |
| R76 | 4.45 | Lamberti | *Hibolithes* sp. | 41.05 | 2436 | 1205 | 3 | 16 | 1.2 | 3.16 |
| R83 | 4.35 | Lamberti | *Hibolithes* sp. | 38.58 | 2985 | 1158 | 3 | 7 | 0.95 | 2.07 |
| R 150 | 4.4 | Lamberti | *Cylindroteuthis* sp. | 39.25 | 1023 | 928 | 1 | 7 | 1.97 | 2.59 |
| R115 | 4.3 | Lamberti | *Hibolithes* sp. | 40.00 | 3280 | 1326 | 12 | 7 | 0.68 | 1.65 |
| R41a | 3.9 | Lamberti | *Hibolithes* sp. | 39.03 | 2993 | 1315 | 5 | 7 | 0.48 | 2.75 |
| R41b | 3.9 | Lamberti | *Hibolithes* sp. | 40.03 | 2661 | 1247 | 5 | 41 | 0.88 | 2.38 |

## 7. Discussion

### 7.1. Oxygen isotopes, Mg/Ca and Sr/Ca ratios

Disequilibrium fractionation of oxygen isotopes during precipitation of biogenic carbonates is caused by a kinetic effect, which relies on the discrimination against heavy oxygen and carbon isotopes during hydration and hydroxylation of $CO_2$ (McConnaughey, 1989; McConnaughey et al., 1997). Kinetic isotope fractionation is consequently reflected in a simultaneous depletion in $^{18}O$ and $^{13}C$ isotopes and a significant linear correlation of $\delta^{18}O$ and $\delta^{13}C$ values. A lack of such correlations in our data sets (cf. Figs. 6, 9) suggests that belemnite rostra and ammonite shells were precipitated in the oxygen isotopic equilibrium with seawater.

Belemnite calcite is normally considered to have been precipitated in oxygen isotope equilibrium with ambient seawater (Niebuhr and Joachimski, 2002; Price and Rogov, 2009; Price and Sellwood;, 1997; Rosales et al., 2004; Sælen et al., 1996; Wierzbowski, 2002; Wierzbowski and Joachimski, 2007). This assumption is substantiated by equilibrium precipitation of oxygen isotopes in the cuttlebone of modern *Sepia*, which

**Table 2**
Age, taxonomy, preservation of microstructure and isotope ratios of ammonite and trigoniid shells. All samples consist of >99% aragonite. Isotope ratios in ‰ relative to VPDB.

| Sample No. | Position (m) | Subzone | Taxonomy | Microstructure | $\delta^{18}O$ (‰) | $\delta^{13}C$ (‰) |
|---|---|---|---|---|---|---|
| R78bis | 6 | Scarburgense/Praecordatum | *Cardioceras* ? | Altered | 1.46 | 3.92 |
| R146/1 | 5.8 | Scarburgense | *Cardioceras* ? | Altered | −0.07 | 3.61 |
| R146/2 | 5.8 | Scarburgense | *Cardioceras* ? | Altered | −0.06 | 3.45 |
| R48/1 | 5.75 | Scarburgense | *Cardioceras* ? | Well-preserved | 1.07 | 2.7 |
| R48/2 | 5.75 | Scarburgense | *Cardioceras* ? | Well-preserved | 0.89 | 2.62 |
| R127/1 | 5.75 | Scarburgense | ammonite | Altered | 0.43 | 4.1 |
| R127/2 | 5.75 | Scarburgense | ammonite | Altered | 0.43 | 4.05 |
| R139 | 5.75 | Scarburgense | *Cardioceras* sp. | Well-preserved | 0.93 | 3.28 |
| R140 | 5.65 | Scarburgense | *Vertumniceras* sp. | Well-preserved | 0.65 | 4.86 |
| R81 | 5.55 | Scarburgense | *Cardioceras* sp. | Well-preserved | 0.41 | 2.67 |
| R133/2 | 5.35 | Scarburgense | *Euaspidoceras* sp. | Altered | −0.05 | 3.36 |
| R105a/1 | 5.25 | Scarburgense | *Euaspidoceras* sp. | Altered | 0.09 | 3.74 |
| R105a/2 | 5.25 | Scarburgense | *Euaspidoceras* sp. | Altered | 0.17 | 3.51 |
| R51 | 5.25 | Scarburgense | *Cardioceras* sp. | Well-preserved | 0.32 | 4.09 |
| R105b/1 | 5.25 | Scarburgense | *Trigonia* sp. | Altered | 0.29 | 3.35 |
| R105b/2 | 5.25 | Scarburgense | *Trigonia* sp. | Altered | 0.61 | 3.59 |
| R82 | 5.2 | Lamberti/Scarburgense | *Cardioceras* sp. | Well-preserved | 1.01 | 4.09 |
| R122/1 | 5.2 | Lamberti/Scarburgense | *Quenstedtoceras* sp. | Well-preserved | 0.95 | 1.95 |
| R55/1 | 5.15 | Lamberti | *Quenstedtoceras* sp. | Altered | 0.25 | 3.94 |
| R55/2 | 5.15 | Lamberti | *Quenstedtoceras* sp. | Altered | −0.09 | 3.72 |
| R70/1 | 5.15 | Lamberti | *Euaspidoceras* sp. | Altered | 0.24 | 3.83 |
| R70/2 | 5.15 | Lamberti | *Euaspidoceras* sp. | Altered | 0.26 | 3.45 |
| R107/1 | 5.15 | Lamberti | *Euaspidoceras* sp. | Altered | 0.10 | 3.75 |
| R107/2 | 5.15 | Lamberti | *Euaspidoceras* sp. | Altered | 1.04 | 3.88 |
| R44/1 | 5 | Lamberti | *Quenstedtoceras* sp. | Altered | 0.37 | 3.71 |
| R57/1 | 4.85 | Lamberti | *Trigonia* sp. | Altered | 0.63 | 3.49 |
| R57/2 | 4.85 | Lamberti | *Trigonia* sp. | Altered | 0.53 | 3.75 |
| R112/1 | 4.85 | Lamberti | *Quenstedtoceras* sp. | Altered | 0.88 | 4.29 |
| R112/2 | 4.85 | Lamberti | *Quenstedtoceras* sp. | Altered | 1.02 | 4.27 |
| R73/1 | 4.75 | Lamberti | *Quenstedtoceras* sp. | Altered | −1.09 | 2.65 |
| R73/2 | 4.75 | Lamberti | *Quenstedtoceras* sp. | Altered | −1.03 | 2.74 |
| R93/1 | 4.75 | Lamberti | *Quenstedtoceras* ? | Well-preserved | 1.29 | 3.92 |
| R108 | 4.75 | Lamberti | *Quenstedtoceras* sp. | Altered | 0.49 | 3.61 |
| R49/1 | 4.65 | Lamberti | *Euaspidoceras* sp. | Altered | −1.56 | 3.91 |
| R49/2 | 4.65 | Lamberti | *Euaspidoceras* sp. | Altered | −1.68 | 3.87 |
| R54 | 4.45 | Lamberti | *Trigonia* sp. | Altered | 0.55 | 3.9 |
| R100 | 4.3 | Lamberti | *Sublunuloceras* sp. | Well-preserved | 0.88 | 2.77 |
| R97 | 4.25 | Lamberti | *Aligaticeras* sp. | Altered | −0.66 | 3.61 |
| R119 | 4.25 | Lamberti | *Sublunuloceras* sp. | Well-preserved | −0.09 | 1.41 |
| R111/1 | 4.15 | Lamberti | *Sublunuloceras* sp. | Well-preserved | 0.18 | 2.27 |
| R111/2 | 4.15 | Lamberti | *Sublunuloceras* sp. | Well-preserved | 0.13 | 2.17 |
| R47 | 3.55 | Lamberti | *Quenstedtoceras* sp. | Altered | −0.64 | 4.10 |
| R94/1 | 3.3 | Lamberti | *Peltoceras* sp. | Altered | −0.06 | 3.18 |
| R94/2 | 3.3 | Lamberti | *Peltoceras* sp. | Altered | 0.03 | 3.00 |
| R88 | 3.2 | Lamberti | *Quenstedtoceras* sp. | Altered | 0.59 | 4.31 |

is a close relative of belemnites (Bettencourt and Guerra, 1999; Rexfort and Mutterlose, 2006; Wefer and Berger, 1991). Belemnopseid and cylindroteuthid belemnites are interpreted to have been nektobenthic as their oxygen isotope records are similar to the records of brachiopods and bivalves (Anderson et al., 1994; Wierzbowski, 2002; Wierzbowski and Joachimski, 2007). Studies of recent *Nautilus*, a relative of ammonites, prove that its oxygen isotope composition is a reliable proxy for the temperature of ambient seawater (Auclair et al., 2004; Landman et al., 1994; Taylor and Ward, 1983). Jurassic ammonites are commonly interpreted to have lived nektonically in the upper part of the water column based on isotope data (Anderson et al., 1994; Lécuyer and Bucher, 2006; Lukeneder et al., 2010; Martill et al., 1994). A near-surface water habit is also suggested for the members of the families Cardioceratidae and Oppeliidae (Price and Page, 2008; Wierzbowski and Joachimski, 2007). The migration of ammonites into shallower and warmer waters during adult life stages has been recently suggested based on internal variations in ammonite isotope ratios (Lukeneder et al., 2010). The oxygen isotope ratio of studied adult portions of ammonite shells is hence interpreted to be an indicator of the temperature of the upper part of the water column.

Mg/Ca and Sr/Ca ratios of the studied groups of belemnites do not correlate with their $\delta^{18}O$ values (Figs. 10, 11). The absence of the observable correlation may result from the relatively narrow range of $\delta^{18}O$ values measured from specimens of each belemnite group. However, the significant scatter of Mg/Ca ratios of *Hibolithes* probably points to a major role of the biofractionation effects on this ratio. The rostra of *Hibolithes* were reported to show no or only a weak relation between Mg/Ca and oxygen isotope ratios as well as higher Mg contents than the other belemnite genera (McArthur et al., 2004, 2007b). Significant correlation was in contrast observed between both Mg/Ca and Sr/Ca ratios and $\delta^{18}O$ values of other Jurassic and Cretaceous belemnites (cf. McArthur et al., 2000, 2004, 2007a,b; Rosales et al., 2004).

Palaeotemperatures were calculated from $\delta^{18}O$ values of well-preserved cephalopod shells assuming normal marine salinity of the sea in the Saratov area and the $\delta^{18}O$ value of Jurassic seawater to have been −1‰ SMOW as distinctive of an ice-free world (Shackleton and Kennett, 1975). The normal marine salinity was assumed owing to the presence of a stenohaline benthic fauna. Palaeotemperatures calculated for cylindroteuthid belemnites vary from 2.3 to 9.1 °C (average 5 °C). Palaeotemperatures calculated for belemnopseid belemnites vary from 6.8 to 10.7 °C (average 8 °C). Ammonite palaeotemperatures range from 10.1 to 16.6 °C (average 13 °C) although a difference is observed between the temperatures calculated for the cardioceratid (average 12 °C) and the oppeliid ammonites (average 15 °C). It is highly improbable that the low temperatures calculated from nektobenthic belemnites were overestimated owing to a decrease in salinity and

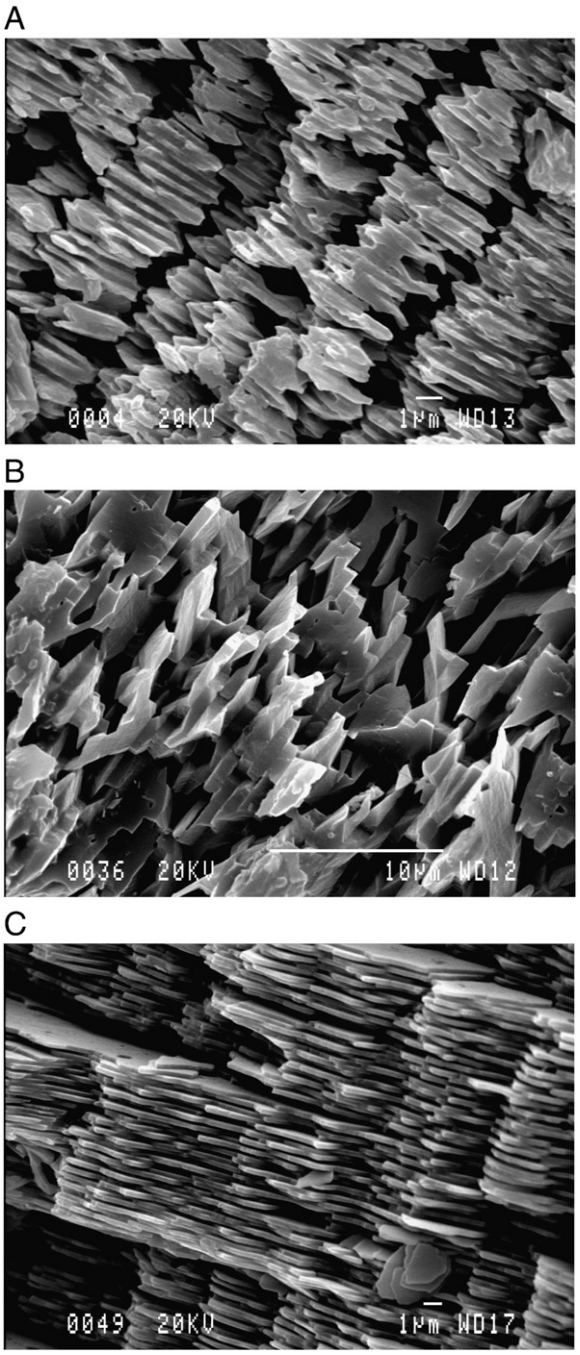


**Fig. 5.** SEM photomicrographs of the nacreous layer of cephalopod shells (>99% aragonite). (A) Dissolution and aggregation of nacreous tablets. *Peltoceras*, sample R94, Lamberti Zone. (B) Dissolution of nacreous tablets. *Trigonia*, sample R54, Lamberti Zone. (C) Well-preserved microstructure of nacreous layer. *Cardioceras*, sample R82, boundary of Lamberti and Mariae zones.

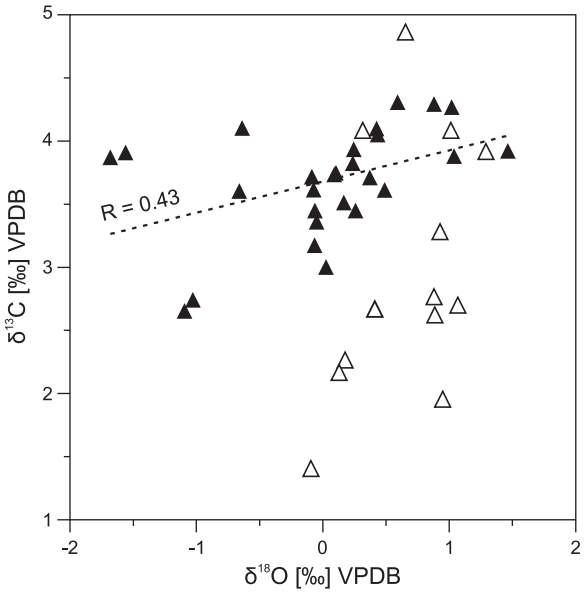


**Fig. 6.** $\delta^{18}O$ and $\delta^{13}C$ values of aragonitic ammonite shells. Open triangles — shells characterized by well-preserved microstructure. Filled triangles — shells characterized by altered microstructure. Positive correlation (significant at 5% level) between $\delta^{18}O$ and $\delta^{13}C$ values of shells with altered microstructure is found.

seawater $\delta^{18}O$ value. The presence of $^{18}O$-enriched seawater is, on the contrary, incompatible with a cool climate. Despite the presence of the stenohaline benthic fauna and the scarcity of the land-derived material the near-surface waters of the basin may have been affected by salinity variations. A decrease in surface water salinity and $\delta^{18}O$ value due to the freshwater influx could result in the overestimation of the palaeotemperatures reconstructed from $\delta^{18}O$ values of nektonic ammonites. The calculated temperature gradient between nektobenthic belemnites (*Hibolithes*) and nektonic ammonites from Dubki is however similar or lesser than the same gradients noted in other Middle–Late Jurassic epicontinental basins of Europe (cf. Anderson et al., 1994; Price and Page, 2008; Wierzbowski and Joachimski, 2007). This may show that the effect of a decrease in surface water salinity on calculated ammonite temperatures is negligible.

The difference in the palaeotemperatures calculated from co-occurring cylindroteuthid and belemnopseid rostra (about 3 °C) may indicate that both nektobenthic belemnite groups inhabited different depth habitats and are found in the same place due to occasional migrations (e.g. for spawning) or as a result of predation. Alternative explanation of belemnite temperature record may be differences in seasonal calcification between cylindroteuthid and belemnopseid belemnites. Slowdown or cessation of growth of belemnopseid rostra during cooler months may account for the observed differences in the belemnite temperature record. Cylindroteuthids are most abundant in two layers (the boundary of the Lamberti and the Mariae Zones and the middle part of the Praecordatum Subzone of the Mariae Zone) and disappear completely starting from the upper part of the Praecordatum Subzone of the Mariae Zone in Dubki. Belemnopseids show higher water temperatures and occur almost continuously throughout the studied interval. Despite the discontinuous occurrence of cylindroteuthids in the studied section the palaeotemperatures calculated for belemnopseids do not change. The same applies to palaeotemperatures calculated from cylindroteuthids in one layer characterized by a scarcity of belemnopseids. These facts likely indicate that both belemnite groups lived separately and inhabited different depths. A similar situation is observed in some areas of modern oceans where different depths and water masses are inhabited by squids of boreal and tropical origin (Arkhipkin and Laptikhovsky, 2006). The belemnites likely did not tolerate a change in environmental conditions. In a case of the change some of them became scarce or disappeared. Two episodes with abundant cylindroteuthids may represent colder periods or periods of the increased flux of cold bottom waters. The retreat of cylindroteuthids may have resulted from the disappearance of cold bottom waters.

The highest temperatures deduced from ammonite $\delta^{18}O$ values are interpreted to record temperatures of near-surface waters. The average temperature (12 °C) for cardioceratids, which were collected from the uppermost part of the Lamberti Subzone of the Lamberti Zone and the Scarburgense Subzone of the Cordatum Zone, and the

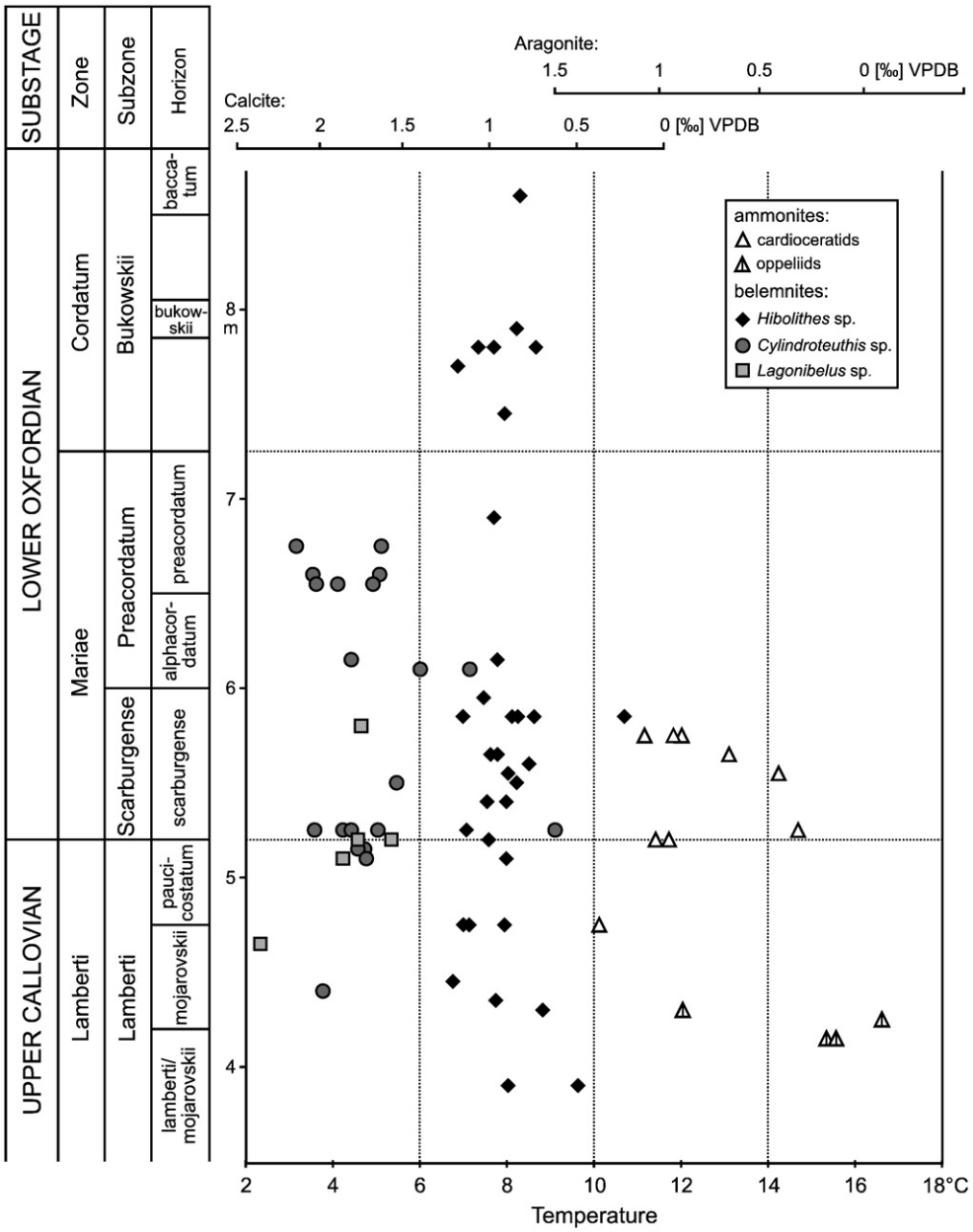


**Fig. 7.** Stratigraphy, $\delta^{18}O$ values and palaeotemperatures calculated from $\delta^{18}O$ values of well-preserved belemnite rostra and ammonite shells from the Dubki section using equations given by O'Neil et al. (1969) and modified by Friedman and O'Neil (1977) for calcite and Grossman and Ku (1986) for molluscan aragonite.

average temperature (15 °C) for oppeliids, which were collected from the lower part of the Lamberti Subzone of the Lamberti Zone, differ either due to partly different lifestyles of two ammonite groups or temporal changes in the temperatures of near-surface waters.

Low temperatures (3–10 °C; the temperatures were recalculated using O'Neil et al.'s, 1969 equation modified by Friedman and O'Neil, 1977) deduced from oxygen isotope composition of uppermost Callovian–lowermost Oxfordian belemnite rostra from the Russian Platform were given as an evidence for global cooling and glaciation at the Middle–Upper Jurassic transition (Dromart et al., 2003a; Price and Rogov, 2009). The present data, however, show a vertical thermal gradient in the water column in the south-central part of the Middle Russian Sea at the Middle–Late Jurassic transition (late Lamberti and early Mariae chrons). The temperatures of deep bottom waters of the sea were likely close to 5 °C (average for cylindroteuthids) being similar to the temperature of modern intermediate waters, which form in cool subpolar regions. Near-surface waters of the sea were likely much higher and averaged 12–15 °C although one cannot completely exclude that the temperatures are slightly overestimated due to a decrease in salinity and $\delta^{18}O$ value of surface water.

The calculated temperatures of sea-bottom waters of the Middle Russian Sea near Saratov (cylindroteuthid and belemnopseid averages of 5 and 8 °C) are lower than the average belemnite temperatures (11 and 12 °C) reported from the Lamberti and the Bukowskii subzones of the Lamberti and the Cordatum zones, respectively, from the Polish Jura Chain (Wierzbowski et al., 2009); the belemnite average temperature (12 °C, the temperature was recalculated using O'Neil et al.'s, 1969 equation modified by Friedman and O'Neil, 1977) of the Lamberti and the Mariae zones from Dorset in England (Price and Page, 2008) and a little lower than the belemnite average temperatures (7 and 10 °C, the temperatures were recalculated using O'Neil et al.'s, 1969 equation modified by Friedman and O'Neil, 1977) of the

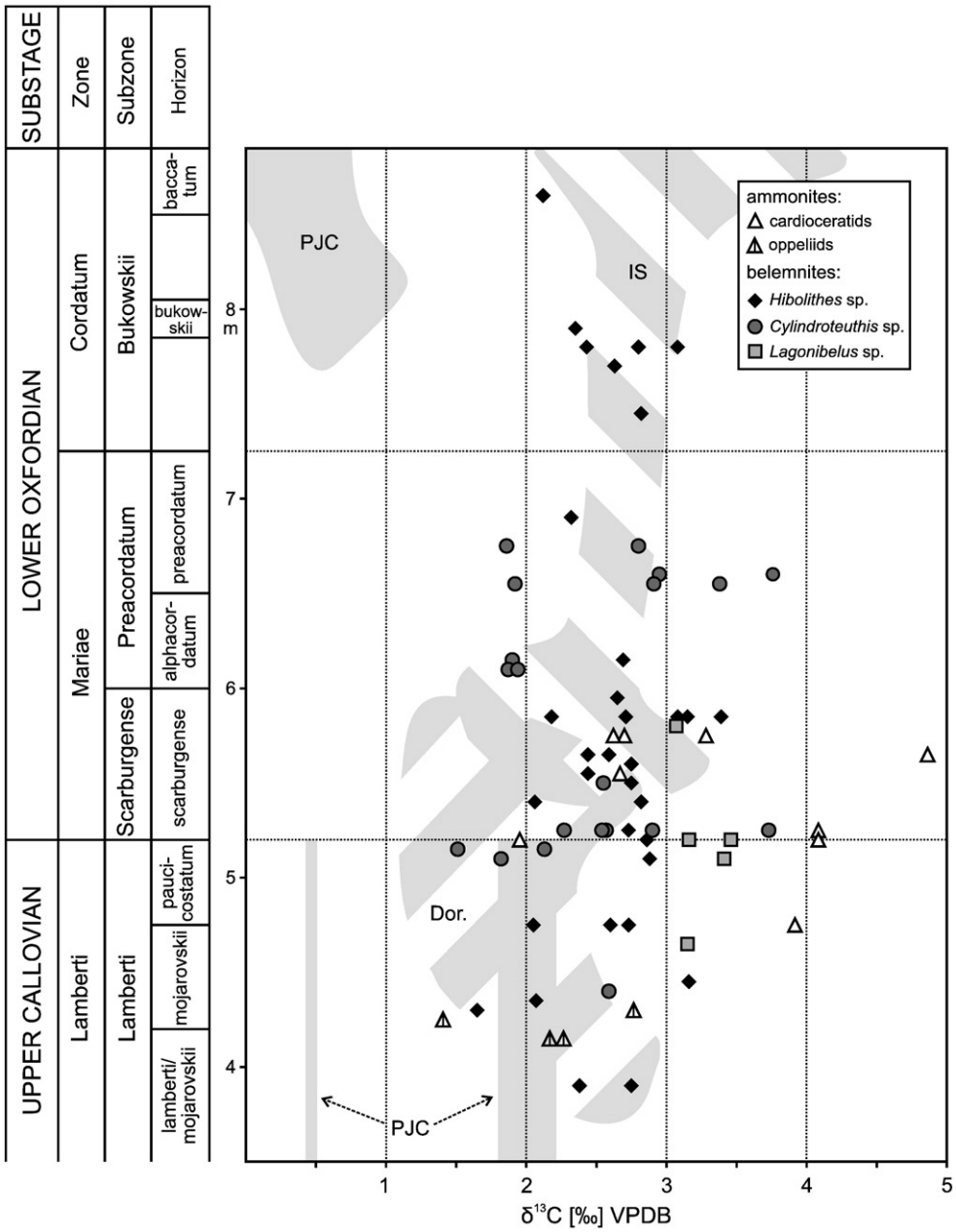


**Fig. 8.** Stratigraphy and $\delta^{13}C$ values of well-preserved belemnite rostra and ammonite shells from the Dubki section and literature $\delta^{13}C$ data. Uniformly grey area corresponds to belemnite $\delta^{13}C$ values from the Polish Jura Chain, Poland (after Wierzbowski et al., 2009), lower striped area corresponds to belemnite $\delta^{13}C$ values from Dorset, England (after Price and Page, 2008), upper striped area corresponds to belemnite $\delta^{13}C$ values from the Isle of Skye, Scotland (after Nunn et al., 2009).

Mariae Zone and the Bukowskii Subzone of the Cordatum Zone, respectively, from the Isle of Skye in Scotland (Nunn et al., 2009). The calculated near-surface temperatures of the sea of the Middle Russian Sea (cardioceratid and oppeliid averages of 12 and 15 °C) are in turn lower than the cardioceratid average temperature (16 °C, the temperature were recalculated using the equation of Grossman and Ku, 1986 established for "mollusks") of the Lamberti and the Mariae Zones from Dorset in England (Price and Page, 2008) and the temperatures (17 and 19 °C, the postulated ice-effect on seawater $\delta^{18}O$ value was rejected; cf. Wierzbowski et al., 2009) of surface or near-surface waters obtained from nektonic fish teeth of the Lamberti–Mariae zones from eastern France and western Switzerland (Dromart et al., 2003a,b).

The review of presented data shows climatic zonation in European seas at the Middle–Late Jurassic transition. The Middle Russian Sea was likely affected by the circulation of cold bottom waters during the latest Callovian and the earliest Oxfordian and predominantly settled by Boreal–Subboreal ammonite fauna. The cold bottom waters might have temporarily spread to the area of Scotland, which was settled as well by Boreal–Subboreal fauna, especially during the Mariae Chron (cf. Nunn et al., 2009) but did not spread further to the south to the areas of Dorset and the Polish Jura Chain (see Fig. 2) as shown with higher temperatures calculated from $\delta^{18}O$ values of belemnite rostra from these regions (cf. Price and Page, 2008; Wierzbowski et al., 2009). The latter regions were characterized by more diverse ammonite fauna of Subboreal and Submediterranean affinities (Matyja and Giżejewska, 1979; Page et al., 2009). The cold bottom waters may have originated in cool Arctic regions during the Jurassic (cf. Sellwood and Valdes, 2008) and affected the Middle Russian Sea flowing through the relatively wide Mezen–Pechora straits (Fig. 2). Despite low temperatures of bottom waters the temperatures of near-surface waters of the Middle Russian Sea were likely higher than it was previously assumed.

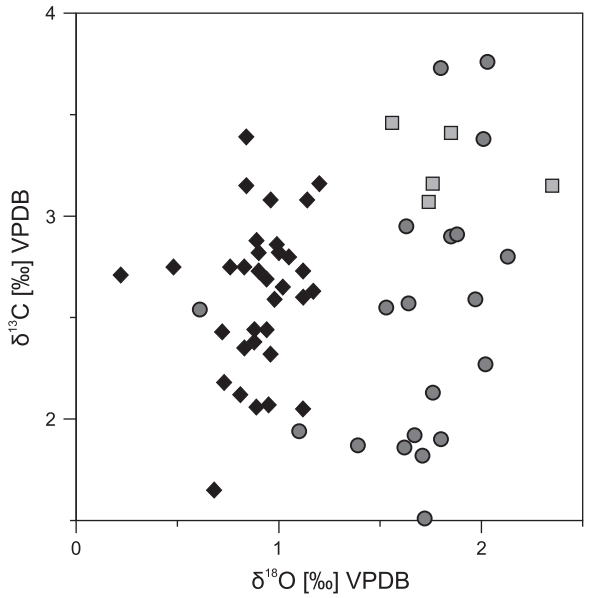


**Fig. 9.** $\delta^{18}O$ versus $\delta^{13}C$ values. Black diamonds — *Hibolithes* sp., grey circles — *Cylindroteuthis* sp., grey squares — *Lagonibelus* sp.. No correlation between $\delta^{18}O$ and $\delta^{13}C$ values is observed.

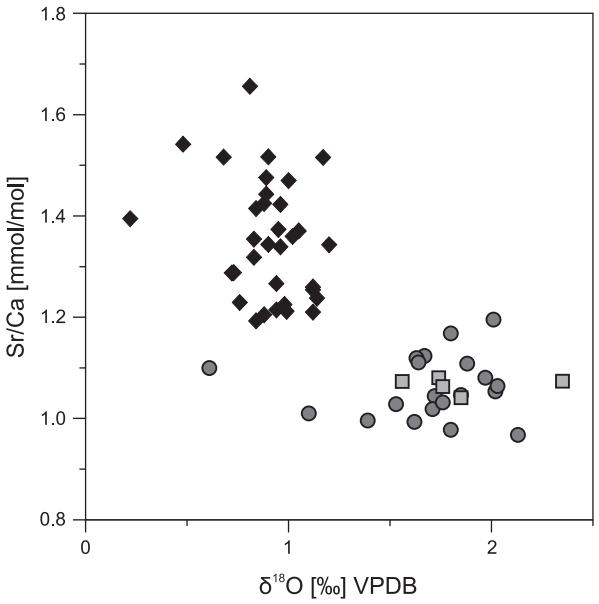


**Fig. 11.** Sr/Ca ratios versus $\delta^{18}O$ values of well-preserved belemnite rostra. Symbols as in Fig. 9. No correlation between Sr/Ca ratios and $\delta^{18}O$ values is observed.

### 7.2. Variations in faunal assemblages and palaeoclimate

Variations in the distribution of belemnites in the Dubki section only partially correlate with quantitative variations in ammonite assemblages. A cylindroteuthid-dominated interval at the boundary of the Lamberti and the Mariae Zones corresponds well to the maximal increase in the percentage of Boreal cardioceratids in Dubki at the Callovian–Oxfordian transition (Figs. 7, 12). The increase in the number of cardioceratid ammonites at the Callovian–Oxfordian transition is widely known and observed e.g. in the Mikhailov section of Ryazan region of Russia and in France (Fortwengler et al., 1997; Vidier et al., 1993; Figs. 2, 12). A higher interval with abundant cylindroteuthids in the Praecordatum Subzone of the Mariae Zone in the Dubki section correlates, on the contrary, with a slight retreat of cardioceratids and a slight increase in the percentage of aspidoceratids and perisphinctids (Figs. 7, 12). The cardioceratid-dominated interval at the base of the Bukowskii Subzone of the Cordatum Zone in Dubki is in turn characterized by the total lack of cylindroteuthids and scatter findings of *Hibolithes* (Figs. 7, 12). The absence of a direct correlation between the belemnite distribution (and the belemnite isotope record) and relative abundances of Boreal cardioceratid ammonites in the Dubki section could be explained by different depth habitats of ammonites and belemnites as discussed above.

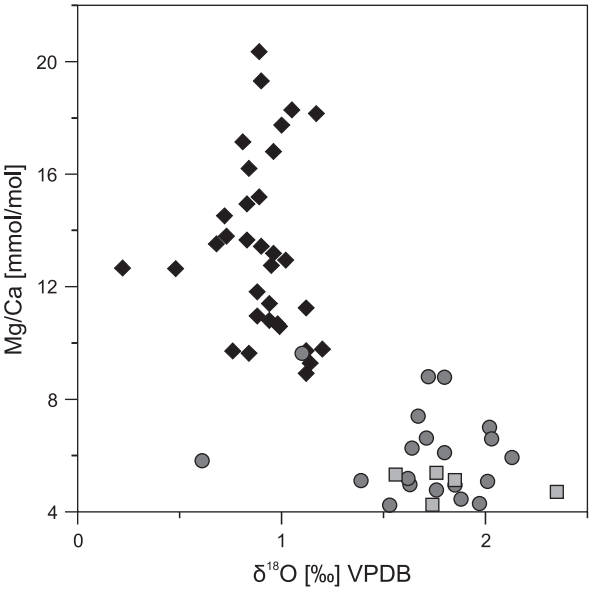


**Fig. 10.** Mg/Ca ratios versus $\delta^{18}O$ values of well-preserved belemnite rostra. Symbols as in Fig. 9. No correlation between Mg/Ca ratios and $\delta^{18}O$ values is observed.

Interestingly, the uppermost part of the Dubki section, belonging to the baccatum horizon of the Bukowskii Subzone of the Cordatum Zone, is marked by sudden increase in the number of Mediterranean oppeliid ammonites (Fig. 12). The *Taramelliceras*-dominated assemblage (up to ~90%) of the baccatum horizon of the Dubki section is unique to the Lower Oxfordian of the whole Subboreal Province. A similar *Taramelliceras*-dominated assemblage has only been recognized in the Cordatum Subzone of the Cordatum Zone of SE France (Quereilhac et al., 2009). In central Poland *Taramelliceras* only attain ~18% of the whole ammonite assemblage of the Cordatum Zone (Tarkowski, 1990). Lower Oxfordian oppeliid ammonites were reported from Mangyshlak (Repin and Rashvan, 1996) and from Samara region of the Volga Basin (Sintzov, 1888) but in the Moscow area these ammonites become very rare. Mass occurrence of *Taramelliceras* in the baccatum horizon of the Dubki section may be linked to the influence of southern water current. The onset of oppeliids in Dubki and significant retreat of cardioceratids from this section are preceded by the retreat of cylindroteuthid belemnites, which disappear in the upper part of the Praecordatum Subzone of the Mariae Zone. The changes in belemnite and ammonite fauna are likely concomitant with major perturbations in ostracod assemblage observed in the upper part of the Dubki section by Tesakova (2008). They may arise because of changing environment conditions and the shallowing of the basin (cf. Tesakova, 2008). Unfortunately, the lack of well-preserved ammonite shells in the upper part of the Dubki section (upper part of the Mariae Zone and the Cordatum Zone) disables the reconstruction of the temperature of near-surface waters.

The existence of a prolonged period of global glaciation at the Middle–Late Jurassic transition was recently questioned by Wierzbowski et al. (2009) but a shorter cooling period might have occurred during the Mariae Chron (cf. Nunn et al., 2009; Wierzbowski et al., 2009). It is also possible that a specific sea water circulation during the latest Callovian–earliest Oxfordian sea-level highstand (cf. Hallam, 2001; Norris and Hallam, 1995; Wierzbowski et al., 2009) may have resulted in the

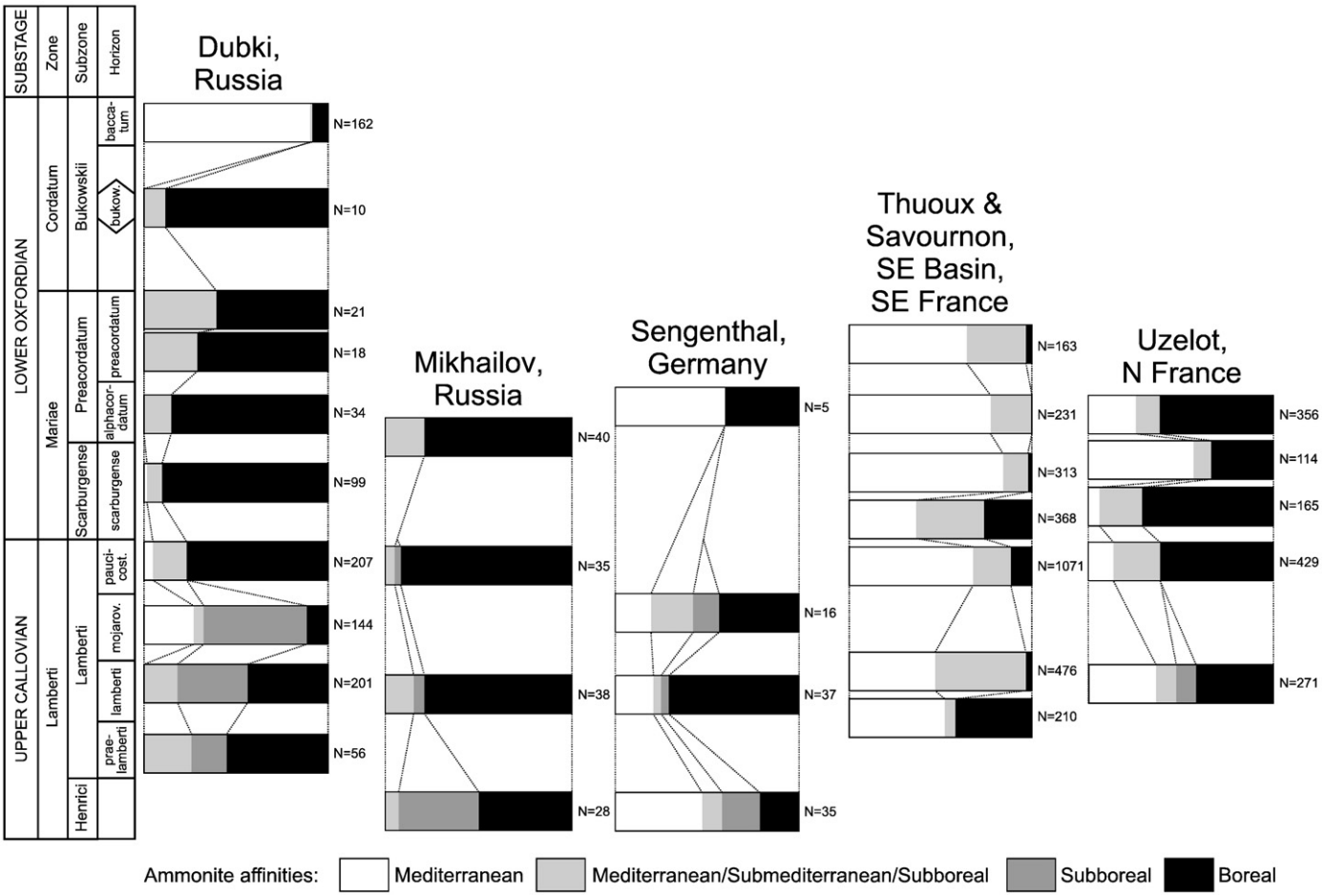


**Fig. 12.** Changes in ammonite assemblages through the Callovian–Oxfordian boundary of different regions: Dubki section; Mikhailov section — Ryazan region of Russia (unpublished data of the authors); Sengenthal section — southern Germany (after Pappler et al., 1982; biostratigraphic interpretation of this section is revised); composite Thuoux, Savournon and SE Basin section — SE France (after Fortwengler et al., 1997, simplified; kosmoceratids are mentioned in body of text but absent in ammonite spectra); Uzelot section — Boulonnais area of northern France (after Vidier et al., 1993, simplified). Ammonites are ranged by their affinities (after Page et al., 2009): Mediterranean — Oppeliidae, Haploceratidae, Phylloceratina and Lytoceratina; Mediterranean/Submediterranean/Subboreal — Aspidoceratidae, Perisphinctidae; Subboreal — Kosmoceratidae; Boreal — Cardioceratidae. N — number of specimens within the assemblage.

incursion of Arctic waters into the Middle Russian Sea and the appearance of a cold bottom current flowing southward to the Tethys (Fig. 2). This current may have disappeared during the Early–Middle Oxfordian as a result of marine regression and the appearance of barriers preventing water exchange. The shallowing and the change in water circulation in the Saratov area of the Middle Russian Sea during the Early Oxfordian were likely accompanied by the reduction in the abundance and the homogeneity of ostracod assemblage (Tesakova, 2008), the retreat of cylindroteuthid belemnites and the onset of oppeliid ammonites. The gradual shallowing and an increased flux of freshwater may have also led to a strong rise of temperatures calculated from belemnite $\delta^{18}O$ values of the Russian Platform in the Oxfordian (cf. Dromart et al., 2003a; Price and Rogov, 2009; Riboulleau et al., 1998). The Oxfordian is marked by a global sea-level fall that occurred after latest Callovian–earliest Oxfordian maximal flooding event (cf. Hallam, 2001; Norris and Hallam, 1995; Wierzbowski et al., 2009). A regressive event was also observed in the latest Early Oxfordian of the Russian Platform although the sea-level fluctuations in this area were considered to be more complex (Sahagian et al., 1996).

It is to emphasise that there is no evidence for the glaciation in northern Siberia and NE Asia at the Callovian–Oxfordian transition as postulated by Dromart et al. (2003a,b). Chumakov and Frakes (1997) showed that Callovian–Oxfordian sediments of the NE Asia, attributed previously to ice-rafting, consist of gravity driven material. Worth noting is also the distribution of glendonites (calcitic pseudomorphs after ikaite) in the Jurassic of Northern Siberia and NE Asia located in the proximity to the palaeo-North Pole. Glendonites are considered to be associated with coldwater-glacial depositional systems as ikaite decomposes rapidly above 4 °C (Selleck et al., 2007). They are abundant in the moderate deep to shallow deposits of the Late Pliensbachian and Aalenian to Bathonian age in the Northern Siberia and NE Asia (Kaplan, 1978; Meledina, 1994; Meledina et al., 1987). The number of observed glendonites in Northern Siberia decreases rapidly starting from the Lower Callovian (they are mainly restricted by lowermost part of the substage) and only one locality with uppermost Middle to lowermost Upper Callovian glendonites — Bolshoi Begichev Island is known (see Kaplan, 1978; Meledina, 1994). Chumakov and Frakes (1997) mentioned another occurrence of glendonites close to the Callovian–Oxfordian transition from the Koster Formation (Artyk river, NE Asia). Unfortunately ammonites from this formation were not figured or described. The macrocephalitid ammonites reported from the upper part of the Koster Formation (Paraketsov and Paraketsova, 1989) suggests, however, its early Bathonian age, because only the ammonites of the *Arctocephalites–Arcticoceras* lineage, which may be misidentified with macrocephalitids, are present in this area (cf. Kiselev and Rogov, 2007). The same applies to the reported presence of *Quenstedtoceras* in the Koster Formation (cf. Paraketsov and Paraketsova, 1989) as true *Quenstedtoceras*, except for *Q.* (*Soaniceras*) that can be easily distinguished from *Quenstedtoceras* s.s., are unknown from NE Asia (see Meledina, 1994). It

is therefore possible that some microconchs of Bathonian or Callovian cardioceratids (*Pseudocadoceras* s.l.) were misidentified with *Quenstedtoceras*, which led to improper dating of the NE Asia sediments.

### 7.3. Carbon isotopes

Metabolic fractionation of carbon isotopes was reported for modern Sepia (Bettencourt and Guerra, 1999; Rexfort and Mutterlose, 2006). The study of Wierzbowski (2002) showed a constant offset in $\delta^{13}C$ values of 2.5 to 3‰ between coeval belemnite and brachiopod calcite with the belemnopseid rostra being depleted in $^{13}C$. Carbon isotope ratios of the belemnopseid belemnite rostra are hence interpreted to be affected by vital fractionation (Wierzbowski, 2002; Wierzbowski and Joachimski, 2007). Despite the metabolic effect the belemnite $\delta^{13}C$ values are found to be a reliable proxy for temporal changes of the isotope composition of the dissolved inorganic carbon (DIC) in ancient seas (cf. Gröcke et al., 2003; McArthur et al., 2000; Price et al., 2000; Rosales et al., 2001; Wierzbowski, 2002; Wierzbowski, 2004; Wierzbowski and Joachimski, 2007).

Non-equilibrium carbon isotope fractionation was reported for the modern *Nautilus macromphalus* (Auclair et al., 2004). The offset from expected equilibrium values may be deduced from the mean $\delta^{13}C$ value of shell aragonite (+0.5‰ VPDB; Auclair et al., 2004), the average $\delta^{13}C$ value of seawater DIC (+0.5‰ VPDB; Auclair et al., 2004) and the aragonite–$HCO^{3-}$ carbon isotope fractionation of + 2.7‰ (Romanek et al., 1992). The vital fractionation effect of around 2.7‰ is calculated with these values. The large metabolic bias in $\delta^{13}C$ values of *N. macromphalus* implies that vital fractionation might have been effective as well during precipitation of ammonite shells.

A significant scatter of coeval $\delta^{13}C$ values of belemnite rostra and ammonite shells (Fig. 8) may result from short-lived temporal changes in the isotope composition of DIC in the epicontinental Middle Russian Sea or the presence of migratory cephalopod fauna. The variations in biologic productivity of the shallow Middle Russian Sea may account for the temporal changes in the isotope composition of DIC. The similarity in the $\delta^{13}C$ values of belemnopseid and cylindroteuthid belemnites (the latter are a bit more scattered) indicates that both belemnite groups were characterized by similar metabolic bias of the carbon isotope composition. The $\delta^{13}C$ values of cylindroteuthid and belemnopseid belemnites may thus be compared with each other.

The $\delta^{13}C$ values of Russian belemnites, which range from +1.5‰ to +3.8‰ (average 2.6‰), are similar or significantly higher than the values of belemnopseid belemnites of the Lamberti Subzone of the Lamberti Zone (average of 1.7‰) and the Bukowskii Subzone of the Cordatum Zone (average 0.4‰), respectively, from the Polish Jura Chain (Wierzbowski et al., 2009; Fig. 8). The $\delta^{13}C$ values of Russian belemnites are comparable to the values of belemnopseid belemnites (average 2.0‰) of the Lamberti and the Mariae zones from Dorset in England (Price and Page, 2008) and very similar to the $\delta^{13}C$ values of cylindroteuthid belemnites (averages of 2.4 and 3.0‰) of the Mariae Zone and the Bukowskii Subzone of the Cordatum Zone, respectively, from the Isle of Skye in Scotland (Nunn et al., 2009; Fig. 8). They also are similar to previously published carbon isotope data of the Lamberti and the Mariae zones from the Russian Platform (cf. Barskov and Kiyashko, 2000; Podlaha et al., 1998). 1–2‰ higher $\delta^{13}C$ values of Lower Oxfordian belemnite rostra from Boreal–Subboreal sections in the Russian Platform and Scotland (when compared to belemnites from the Submediterranean ammonite province from Poland) indicate regional enrichment of DIC in $^{13}C$ and the paucity of seawater mixing processes. An 1–2.5‰ offset in $\delta^{13}C$ values between the belemnite rostra from the Submediterranean and the Boreal–Subboreal provinces was observed as well during the Oxfordian and the Early Kimmeridgian in Europe (Wierzbowski, 2004). Callovian–Oxfordian deposits from Boreal–Subboreal basins of Europe are organic-carbon rich. They are interpreted to have been deposited under high nutrient supply and/or conditions favourable for the preservation of organic matter (Bushnev et al., 2006; Martill et al., 1994; Marynowski and Zatoń, 2010; Smirnova et al., 1999; Tyson et al., 1979). The regional enrichment of DIC in $^{13}C$ in restricted Boreal–Subboreal basins may thus be linked to the high organic matter productivity and/or burial under insufficient mixing of water masses. This phenomenon may have been accelerated during the Oxfordian sea-level fall (cf. Hallam, 2001; Norris and Hallam, 1995; Wierzbowski et al., 2009).

The lack of temporal trend in the belemnite $\delta^{13}C$ values from the Dubki section indicates that $\delta^{13}C$ values of DIC in central part of the Middle Russian Sea were high, albeit noisy, throughout the latest Callovian and the earliest Oxfordian. The carbon isotope record of the Dubki section near Saratov is similar to the record of other Boreal–Subboreal localities characterized by high belemnite $\delta^{13}C$ values in the studied time period (cf. Nunn et al., 2009; Price and Page, 2008; Fig. 8). Additional studies are, however, necessary to precisely document carbon isotope variations in the Cordatum Zone of the Russian Platform.

## 8. Conclusions

This study presents high resolution oxygen and carbon isotope records of the Callovian–Oxfordian boundary of the Russian Platform at Saratov based on well-preserved belemnite rostra and ammonite shells. Oxygen and carbon isotope compositions of belemnite rostra and ammonite shells are assumed to be reliable proxies for seawater palaeotemperatures and secular variations in the isotope composition of DIC. Belemnites and ammonites are considered to have been nektobenthic and nektonic dwellers, respectively.

Palaeotemperatures calculated for cylindroteuthid belemnites (average 5 °C), belemnopseid belemnites (average 8 °C) and ammonites (average 13 °C) indicate a vertical thermal gradient within the water column. Low temperatures of bottom waters likely indicate that the Middle Russian Sea was affected by circulation of cold polar waters during the Callovian–Oxfordian transition. It is shown by a comparison of isotope data from various European localities that the cold bottom waters did not spread further to the south to the areas of Poland and England.

The absence of direct correlation between the belemnite oxygen isotope record and the relative abundances of ammonite families in the Dubki section is explained by different depth habitats of ammonites and belemnites. Variations in ammonite, belemnite and ostracod assemblages in the upper part of the Dubki section correlate with each other and may arise because of a change in water circulation in the Saratov area of the Middle Russian Sea during the Early Oxfordian.

There is no evidence for glaciation at the Callovian–Oxfordian transition in Northern Siberia and NE Asia. Spreads of cold bottom waters and cardioceratid ammonite fauna at the Callovian–Oxfordian transition were likely connected with changes in water circulation and palaeogeography of marine basins during sea-level highstand.

The belemnite $\delta^{13}C$ values from the entire study interval are characterized by a significant scatter (+1.5 to +3.8‰) with no distinguishable temporal trend. The Lower Oxfordian carbon isotope record of the Russian Platform at Saratov is similar to the record of the Boreal–Subboreal carbonates but markedly differs from the record of carbonates from the Submediterranean ammonite province. Higher (than Submediterranean) $\delta^{13}C$ values of Lower Oxfordian belemnite rostra from the Boreal–Subboreal ammonite province likely result from high organic matter productivity and/or burial in semi-isolated northern seas.

## Acknowledgements

This study was supported by RFBR grants no. 03-05-64264 and 09-05-00456, the programs no. 16 and 24 of the Presidium of the

Russian Academy of Sciences as well as the statutory funds of the Institute of Geological Sciences, Polish Academy of Sciences. Field work was financed under the agreement on scientific cooperation between the Polish Academy of Sciences and the Russian Academy of Sciences. We are indebted to Dr. S. Yu. Maleonkina from the Geological Institute of RAS, Moscow as well as Prof. A. Yu. Guzhikov and Dr. A.V. Manikin from Saratov State University for help during field work in Dubki. Two anonymous reviewers are thanked for valuable reviews and suggested improvements.

## References


Anderson, T.F., Arthur, M.A., 1983. Stable isotopes of oxygen and carbon and their application to sedimentologic and paleoenvironmental problems. In: Arthur, M.A., Anderson, T.F., Kaplan, I.R., Veizer, J., Land, L.S. (Eds.), Stable Isotopes in Sedimentary Geology, SEPM Short Course No. 10, Dallas, pp. 1-1–1-151.

Anderson, T.F., Popp, B.N., Williams, A.C., Ho, L.-Z., Hudson, J.D., 1994. The stable isotopic records of fossils from the Peterborough Member, Oxford Clay Formation (Jurassic), UK: palaeoenvironmental implications. J. Geol. Soc. Lond. 151, 125–138.

Arkhipkin, A., Laptikhovsky, V., 2006. Allopatric speciation of the teuthid fauna on the shelf and slope of northwest Africa. Acta Universitatis Carolinae - Geologica 49, 15–19.

Auclair, A.-C., Lécuyer, C., Bucher, H., Sheppard, S.M.F., 2004. Carbon and oxygen isotope composition of *Nautilus macromphalus*: a record of thermocline waters off New Caledonia. Chem. Geol. 207, 91–100.

Barskov, I.S., Kiyashko, S.I., 2000. Thermal regime variations in the Jurassic marine basin of the East European Platform at the Callovian/Oxfordian boundary: evidence from stable isotopes in belemnite rostra. Dokl. Earth Sci. 372, 643–645.

Bettencourt, V., Guerra, A., 1999. Carbon- and oxygen-isotope composition of the cuttlebone of *Sepia officinalis*: a tool for predicting ecological information? Mar. Biol. 133, 651–657.

Boggs, S., Krinsley, D., 2006. Application of Cathodoluminescence Imaging to the Study of Sedimentary Rocks. Cambridge University Press.

Buchardt, B., Weiner, S., 1981. Diagenesis of aragonite from Upper Cretaceous ammonites: a geochemical case-study. Sedimentology 28, 423–438.

Bushnev, D.A., Shchepetova, E.V., Lyyurov, S.V., 2006. Organic geochemistry of Oxfordian carbon-rich sedimentary rocks of the Russian Plate. Lithol. Miner. Resour. 41, 423–434.

Chumakov, N.M., Frakes, L.A., 1997. Mode of origin of dispersed clasts in Jurassic shales, southern part of the Yana-Kolyma fold belt, North East Asia. Palaeogeogr. Palaeoclimatol. Palaeoecol. 128, 77–85.

Craig, H., 1965. The measurement of oxygen isotope paleotemperatures. In: Tongiorgi, E. (Ed.), Proceedings of the Spoleto Conference on Stable Isotopes in Oceanographic Studies and Paleotemperatures, Consiglio Nazionale delle Ricerche, Pisa, pp. 161–182.

Dauphin, Y., Denis, A., 1990. Analyse microstructurale des tests de mollusques du Callovien de Lukow (Pologne) – Comparaison de l'etat de conservation de quelques types structuraux majeurs. Rev. Paléobiol. 9, 27–36.

Dauphin, Y., Denis, A., 1999. Diagenèse comparée des phases minérales et organiques solubles dans les tests aragonitiques de nautiles et d'ammonites. Bull. Soc. Géol. Fr. 170, 355–365.

Doyle, P., 1987. Lower Jurassic–Lower Cretaceous belemnite biogeography and the development of the Mesozoic Boreal Realm. Palaeogeogr. Palaeoclimatol. Palaeoecol. 61, 237–254.

Dromart, G., Garcia, J.-P., Gaumet, F., Picard, S., Rousseau, M., Atrops, F., Lecuyer, C., Sheppard, S.M.F., 2003a. Perturbation of the carbon cycle at the Middle/Late Jurassic transition: geological and geochemical evidence. Am. J. Sci. 303, 667–707.

Dromart, G., Garcia, J.-P., Picard, S., Atrops, F., Lecuyer, C., Sheppard, S.M.F., 2003b. Ice Age at the Middle–Late Jurassic transition? Earth Planet. Sci. Lett. 213, 205–220.

Epstein, S., Buchsbaum, R., Lowenstam, H.A., Urey, H.C., 1953. Revised carbonate-water isotopic temperature scale. Geol. Soc. Am. Bull. 64, 1315–1326.

Fortwengler, D., Marchand, D., Bonnot, A., 1997. Les coupes de Thuoux et de Savournon (SE de la France) et la limite Callovien-Oxfordien. Geobios 30, 519–540.

Friedman, I., O'Neil, J.R., 1977. Compilation of stable isotope fractionation factors of geochemical interest. Data of Geochemistry, 6th edition. Geochemical Survey Professional Paper 440 – KK, pp. KK1–KK12.

Fürsich, F.T., Sykes, R.M., 1977. Palaeobiogeography of the European Boreal Realm during Oxfordian (Upper Jurassic) times: a quantitative approach. Neues Jahrb. Geol. P-A. 155, 137–161.

Gaździcka, E., 1998. Middle Oxfordian Tenuiserratum Zone palaeogeography. In: Dadlez, R., Marek, S., Pokorski, J. (Eds.), Palaeogeographical Atlas of the Epicontinental Permian and Mesozoic in Poland, Państwowy Instytut Geologiczny, Warszawa, plate 51.

Golonka, J., 2004. Plate tectonic evolution of the southern margin of Eurasia in the Mesozoic and Cenozoic. Tectonophysics 381, 235–273.

Gröcke, D.R., Price, G.D., Ruffell, A.H., Mutterlose, J., Baraboshkin, E., 2003. Isotopic evidence for Late Jurassic–Early Cretaceous climate change. Palaeogeogr. Palaeoclimatol. Palaeoecol. 202, 97–118.

Grossman, E.L., Ku, T.-L., 1986. Oxygen and carbon isotope fractionation in biogenic aragonite: temperature effects. Chem. Geol. 59, 59–74.

Hallam, A., 2001. A review of the broad pattern of Jurassic sea-level changes and their possible causes in the light of current knowledge. Palaeogeogr. Palaeoclimatol. Palaeoecol. 167, 23–37.

Kaplan, M.E., 1978. Calcite pseudomorphoses from the Jurassic and Lower Cretaceous deposits of Northern East Siberia. Geol. Geofiz. 19, 62–70 [in Russian].

Keupp, H., Mitta, V.V., 2004. Septenbildung bei *Quenstedtoceras* (Ammonoidea) von Saratov (Russland) unter anomalen Kammerdruckbedingungen. Mitteilungen des Geologisch-Paläontologischen Instituts, Universität Hamburg 88, 51–62.

Kim, S.-T., Mucci, A., Taylor, B.E., 2007. Phosphoric acid fractionation factors for calcite and aragonite between 25 and 75 °C: revisited. Chem. Geol. 246, 135–146.

Kiselev, D., Rogov, M.A., 2005. Zones, subzones and biohorizons of the Upper Callovian and Lower Oxfordian of the European part of Russia. In: Zakharov, V.A., Rogov, M.A., Dzyuba, O.S. (Eds.), First All-Russian Meeting, Jurassic System of Russia: Problems of Stratigraphy and Paleogeography, November 21–22, 2005. Geological Institute of Russian Academy of Sciences, Moscow, pp. 128–134. [in Russian].

Kiselev, D.N., Rogov, M.A., 2007. Stratigraphy of the Bathonian–Callovian boundary deposits in the Prosek Section (Middle Volga Region). Article 1. Ammonites and infrazonal biostratigraphy. Stratigr. Geol. Correl. 15, 485–515.

Kiselev, D., Rogov, M., Guzhikov, A., Pimenov, M., Tesakova, E., Dzyuba, O., 2006. Dubki (Saratov region, Russia), the reference section for the Callovian/Oxfordian boundary. Volumina Jurassica 4, 177–179.

Landman, N.H., Cochran, J.K., Rye, D.M., Tanabe, K., Arnold, J.M., 1994. Early life history of *Nautilus*: evidence from isotopic analyses of aquarium-reared specimens. Paleobiology 20, 40–51.

Lécuyer, C., Bucher, H., 2006. Stable isotope compositions of a late Jurassic ammonite shell: a record of seasonal surface water temperatures in the southern hemisphere? eEarth Discussions 1, 1–19.

Lécuyer, C., Picard, S., Garcia, J.P., Sheppard, S.M.F., Grandjean, P., Dromart, G., 2003. Thermal evolution of Tethyan surface waters during the Middle–Late Jurassic: evidence from $\delta^{18}O$ values of marine fish teeth. Paleoceanography 18, 21-1–21-16.

Louis-Schmid, B., Rais, P., Schaeffer, P., Bernasconi, S.M., Weissert, H., 2007. Plate tectonic trigger of changes in $pCO_2$ and climate in the Oxfordian (Late Jurassic): carbon isotope and modeling evidence. Earth Planet. Sci. Lett. 258, 44–60.

Lukeneder, A., Harzhauser, M., Müllegger, S., Piller, W.E., 2010. Earth Planet. Sci. Lett. 296, 103–114.

Marshall, J.D., 1992. Climatic and oceanographic isotopic signals from the carbonate rock record and their preservation. Geol. Mag. 129, 143–160.

Martill, D.M., Taylor, M.A., Duff, K.L., Riding, J.B., Bown, P.R., 1994. The trophic structure of the biota of the Peterborough Member, Oxford Clay Formation (Jurassic), UK. J. Geol. Soc. Lond. 151, 173–194.

Marynowski, L., Zatoń, M., 2010. Organic matter from the Callovian (Middle Jurassic) deposits of Lithuania: compositions, sources and depositional environments. Appl. Geochem. 25, 933–946.

Matyja, B.A., Giżejewska, M., 1979. Distribution of the Callovian and Lower Oxfordian ammonite faunas in Poland. Acta Geol. Pol. 29, 177–185.

Matyja, B.A., Wierzbowski, A., 1995. Biogeographic differentiation of the Oxfordian and Early Kimmeridgian ammonite faunas of Europe, and its stratigraphic consequences. Acta Geol. Pol. 45, 1–8.

McArthur, J.M., Donovan, D.T., Thirlwall, M.F., Fouke, B.W., Mattey, D., 2000. Strontium isotope profile of the early Toarcian (Jurassic) oceanic anoxic event, the duration of ammonite biozones, and belemnite palaeotemperatures. Earth Planet. Sci. Lett. 179, 269–285.

McArthur, J.M., Mutterlose, J., Price, G.D., Rawson, P.F., Ruffel, A., Thirlwall, M.F., 2004. Belemnites of Valanginian, Hauterivian and Barremian age: Sr-isotope stratigraphy, composition ($^{87}Sr/^{86}Sr$, $\delta^{13}C$, $\delta^{18}O$, Na, Sr, Mg), and palaeo-oceanography. Palaeogeogr. Palaeoclimatol. Palaeoecol. 202, 253–272.

McArthur, J.M., Doyle, P., Leng, M.J., Reeves, K., Williams, C.T., Garcia-Sanchez, R., Howarth, R.J., 2007a. Testing palaeo-environmental proxies in Jurassic belemnites: Mg/Ca, Sr/Ca, Na/Ca, $\delta^{18}O$ and $\delta^{13}C$. Palaeogeogr. Palaeoclimatol. Palaeoecol. 252, 464–480.

McArthur, J.M., Janssen, N.M.M., Reboulet, S., Leng, M.J., Thirlwall, M.F., van de Schootbrugge, B., 2007b. Palaeotemperatures, polar ice-volume, and isotope stratigraphy (Mg/Ca, $\delta^{18}O$, $\delta^{13}C$, $^{87}Sr/^{86}Sr$): the Early Cretaceous (Berriasian, Valanginian, Hauterivian). Palaeogeogr. Palaeoclimatol. Palaeoecol. 248, 391–430.

McConnaughey, T., 1989. $^{13}C$ and $^{18}O$ isotopic disequilibrium in biological carbonates: I. Patterns. Geochim. Cosmochim. Acta 53, 151–162.

McConnaughey, T.A., Burdett, J., Whelan, J.F., Paull, C.K., 1997. Carbon isotopes in biological carbonates: respiration and photosynthesis. Geochim. Cosmochim. Acta 61, 611–622.

Meledina, S.V., 1994. Boreal Middle Jurassic of Russia. Transactions of the United Institute of Geology, Geophysics and Mineralogy, Siberian Branch, Russian Academy of Sciences 819, 1–184 [in Russian].

Meledina, S.V., Nalnyaeva, T.I., Shurygin, B.N., 1987. Yura Enisey-Khatangskogo Progiba. Institut Geologii i Geofiziki SO AN SSSR, Novosibirsk.

Mitta, V., 2003. On the Callovian and Oxfordian boundary beds of the Volga area: Vernadsky Museum-Novitates, 11, pp. 1–21. [in Russian].

Niebuhr, B., Joachimski, M.M., 2002. Stable isotope and trace element geochemistry of Upper Cretaceous carbonates and belemnite rostra (Middle Campanian, north Germany). Geobios 35, 51–64.

Norris, M.S., Hallam, A., 1995. Facies variations across the Middle–Upper Jurassic boundary in Western Europe and the relationship to sea-level changes. Palaeogeogr. Palaeoclimatol. Palaeoecol. 116, 189–245.

Nunn, E.V., Price, G.D., Hart, M.B., Page, K.N., Leng, M.J., 2009. Isotopic signals from Callovian–Kimmeridgian (Middle–Upper Jurassic) belemnites and bulk organic carbon, Staffin Bay, Isle of Skye, Scotland. J. Geol. Soc. Lond. 166, 633–641.

O'Neil, J.R., Clayton, R.N., Mayeda, T.K., 1969. Oxygen isotope fractionation in divalent metal carbonates. J. Chem. Phys. 51, 5547–5558.

Page, K.N., 2008. The evolution and geography of Jurassic ammonoids. Proc. Geol. Assoc. 119, 35–57.

Page, K.N., Meléndez, G., Wright, J.K., 2009. The ammonite faunas of the Callovian–Oxfordian boundary interval in Europe and their relevance to the establishment of an Oxfordian GSSP. Volumina Jurassica 7, 89–99.
Pappler, G., Sadati, M., Zeiss, A., 1982. Biostratigraphische Untersuchungen im Grenzbereich Mittlerer/Oberer Jura im Steinbruch Sengenthal/Opf. Geol. Bl. NO-Bayern 32, 35–44.
Paraketsov, K.V., Paraketsova, G.I., 1989. Stratigrafiya i Fauna Verkhneyurskikh i Nizhnemelovykh Otlozheniy Severo-Vostoka SSSR. Nedra, Moskva.
Podlaha, O.G., Mutterlose, J., Veizer, J., 1998. Preservation of $\delta^{18}O$ and $\delta^{13}C$ in belemnite rostra from the Jurassic/Early Cretaceous successions. Am. J. Sci. 298, 324–347.
Price, G.D., Page, K.N., 2008. A carbon and oxygen isotopic analysis of molluscan faunas from the Callovian-Oxfordian boundary at Redcliff Point, Weymouth, Dorset: implications for belemnite behaviour. Proc. Geol. Assoc. 119, 153–160.
Price, G.D., Rogov, M.A., 2009. An isotopic appraisal of the Late Jurassic greenhouse phase in the Russian Platform. Palaeogeogr. Palaeoclimatol. Palaeoecol. 273, 41–49.
Price, G.D., Sellwood, B.W., 1997. "Warm" palaeotemperatures from high Late Jurassic palaeolatitudes (Falkland Plateau). Ecological, environmental or diagenetic controls? Palaeogeogr. Palaeoclimatol. Palaeoecol. 129, 315–327.
Price, G.D., Ruffell, A.H., Jones, C.E., Kalin, R.M., Mutterlose, J., 2000. Isotopic evidence for temperature variation during the early Cretaceous (late Ryazanian–mid-Hauterivian). J. Geol. Soc. Lond. 157, 335–343.
Quereilhac, P., Marchand, D., Jardat, R., Bonnot, A., Fortwengler, D., Courville, P., 2009. La faune ammonitique des marnes à fossiles ferrugineux de la région de Niort, France (Oxfordien inférieur, Zone à Cordatum, Sous-Zone à Cordatum). Carnets Géol. Artic. 2009 (05), 1–21.
Repin, Yu.S., Rashvan, N.H., 1996. Kelloveyskie Ammonity Saratovskogo Povolzhya i Mangyshlaka. NPO "Mir i semya-95", Sankt-Peterburg.
Rexfort, A., Mutterlose, J., 2006. Stable isotope records from *Sepia officinalis* — a key to understanding the ecology of belemnites. Earth Planet. Sci. Lett. 247, 212–221.
Riboulleau, A., Baudin, F., Daux, V., Hantzpergue, P., Renard, M., Zakharov, V., 1998. Évolution de la paléotemperature des eaux de la plate-forme russe au cours du Jurassique supérieur. C.R. Acad. Sci. IIA 326, 239–246.
Rogov, M., Egorov, E.Yu., 2003. Polymorfism u nekotorykh ranneoksfordskikh Oppeliidae (Ammonoidea) Russkoy platformy. In: Bogdanov, N.A., Vasil'eva, T.I., Verzbitsky, V.E., et al. (Eds.), Sovremennye voprosy geologii. Materialy konferencii 3i Janshinskie chteniya, 26–28 marta 2003 goda. Nauchny Mir, Moskva, pp. 245–248.
Romanek, C.S., Grossman, E.L., Morse, J.W., 1992. Carbon isotopic fractionation in synthetic aragonite and calcite: effects of temperature and precipitation rate. Geochim. Cosmochim. Acta 56, 419–430.
Rosales, I., Quesada, S., Robles, S., 2001. Primary and diagenetic isotopic signals in fossils and hemipelagic carbonates: the Lower Jurassic of northern Spain. Sedimentology 48, 1149–1169.
Rosales, I., Robles, S., Quesada, S., 2004. Elemental and oxygen isotope composition of Early Jurassic belemnites: salinity vs. temperature signals. J. Sed. Res. 74, 342–354.
Sælen, G., Doyle, P., Talbot, M.R., 1996. Stable-isotope analyses of belemnite rostra from the Whitby Mudstone Fm., England. Surface water conditions during deposition of a marine black shale. Palaios 11, 97–117.
Sahagian, D., Pinous, O., Olferiev, A., Zakharov, V., 1996. Eustatic curve for the Middle Jurassic–Cretaceous based on Russian Platform and Siberian stratigraphy: zonal resolution. AAPG Bull. 80, 1433–1458.
Savard, M.M., Veizer, J., Hinton, R., 1995. Cathodoluminescence at low Fe and Mn concentrations: a SIMS study of zones in natural calcites. J. Sed. Res. A65, 208–213.
Sazonova, I.G., Sazonov, N.T., 1967. Paleogeografiya Russkoy Platformy v Yurskoe i Rannemelovoe Vremya, Izdatelstvo "Nedra", Leningrad.
Selleck, B.W., Carr, P.F., Jones, B.G., 2007. A review and synthesis of glendonites (pseudomorphs after ikaite) with new data assessing applicability as recorders of ancient coldwater conditions. J. Sed. Res. 77, 980–991.
Sellwood, B.W., Valdes, P.J., 2008. Jurassic climates. Proc. Geol. Assoc. 119, 5–17.
Shackleton, N.J., Kennett, J.P., 1975. Paleotemperature history of the Cenozoic and initiation of Antarctic glaciation: oxygen and carbon isotope analyses in DSDP sites 277, 279 and 281. Init. Rep. Deep Sea Drilling Proj. 29, 743–755.
Sintzov., I., 1888. Carte Géologique generale de la Russie. Feuille 92. Saratov-Pensa. Mém. Com. Géol. 7, 1–132.
Smirnova, S.B., Shubin, S. V., Barskov, I. S., 1999. Palinokompleksy pogranichnykh otlozheniy sredney i verkhney yury v centralnykh i yuzhnykh rayonakh moskovskoy sineklizy. Vestn. Mosk. Univ., Ser. 4 Geologiya 5, 28–32.
Stevens, C.R., 1973. Jurassic belemnites. In: Hallam, A. (Ed.), Atlas of Palaeobiogeography. Elsevier, Amsterdam – London – New York, pp. 259–274.
Świdrowska, J., Hakenberg, M., Poluhtovič, B., Seghedi, A., Višnâkov, I., 2008. Evolution of the Mesozoic basins on the southwestern edge of the East European Craton (Poland, Ukraine, Moldova, Romania). Studia Geologica Polonica 130, 3–130.
Tarkowski, R., 1990. Les *Taramelliceras* (Ammonitina) de l'Oxfordien inférieur du Jurassique cracovien: valeur stratigraphique. 1st Oxfordian Meeting Zaragoza, 1988: Publ. SEPAZ, 2, pp. 205–221.
Taylor, B.E., Ward, P.D., 1983. Stable isotopic studies of *Nautilus macromphalus* Sowerby (New Caledonia) and *Nautilus pompilus* L. (Fiji). Palaeogeogr. Palaeoclimatol. Palaeoecol. 41, 1–16.
Tesakova, E., 2008. Late Callovian and Early Oxfordian ostracods from the Dubki section (Saratov area, Russia): implications for stratigraphy, paleoecology, eustatic cycles and palaeobiogeography. Neues Jahrb. Geol. P-A. 249, 25–45.
Thierry, J., Barrier, E., Abbate, E., Ait-Ouali, R., Ait-Salem, H., Bouaziz, S., Canerot, J., Elmi, S., Georgiev, G., Guiraud, R., Hirsch, F., Ivanik, M., Le Metour, J., Le Nindre, Y.M., Medina, F., Mouty, M., Nazarevich, Nikishin, A.M., Page, K., Panov, D.L., Pique, A., Poisson, A., Sandulescu, M., Sapunov, I.G., Seghedi, A., Soussi, M., Tarkowski, R.A., Tchoumatchenko, P.V., Vaslet, D., Vishnevskaya, V., Volozh, V.A., Voznezenski, A., Walley, C.D., Wong, T.E., Ziegler, M., Aitbrahim, L., Bergerat, F., Bracene, R., Brunet, M.F., Cadet, J.P., Guezou, J.C., Jabaloy, A., Lepvrier, C., Rimmele, G., De Wever, P., Belaid, A., Bonneau, M., Coutelle, A., Fekirine, B., Guillocheau, F., Julien, M., Kokel, F., Lamarche, J., Mami, L., Mansy, J.L., Mascle, G., Meister, C., Pascal, C., Robin, C., Sihamdi, N., Souhel, A., Stephenson, R., Vera, J.A., Vuks, V.J., Vrielynck, B., Olivet, J.L., 2000a. Middle Callovian (157–155 Ma). In: Dercourt, J., et al. (Ed.), Atlas Peri-Tethys, Paleogeographical Maps, CCGM/CGMW Paris, map 9.
Thierry, J., Abbate, E., Alekseev, A.S., Ait-Ouali, R., Ait-Salem, H., Bouaziz, S., Canerot, J., Georgiev, G., Guiraud, R., Hirsch, F., Ivanik, M., Le Metour, J., Le Nindre, Y.M., Medina, F., Mouty, M., Nazarevich, B., Nikishin, A.M., Page, K., Panov, D.L., Pique, A., Poisson, A., Sandalescu, M., Sapunov, I.G., Seghedi, A., Soussi, M., Tchoumatchenko, P.V., Vaslet, D., Vishnevskaya, V., Volozh, V.A., Voznezenski, A., Walley, C.D., Wong, T.E., Ziegler, M., Barrier, E., Bergerat, F., Bracene, R., Brunet, M.F., Cadet, J.P., Guezou, J.C., Jabaloy, A., Lepvrier, C., Rimmele, G., De Wever, P., Baudin, F., Belaid, A., Bonneau, M., Coutelle, A., Fekirne, B., Guillocheau, F., Hantzpergue, M., Julien, M., Kokel, F., Lamarche, J., Mami, L., Mansy, J.L., Mascle, G., Pascal, C., Robin, C., Stephenson, R., Sihamdi, N., Vera, J.A., Vuks, V.J., 2000b. Early Kimmeridgian (146–144 Ma). In: Dercourt, J., et al. (Ed.), Atlas Peri-Tethys, Paleogeographical Maps, CCGM/CGMW Paris, map 10.
Tyson, R.V., Wilson, R.C.L., Downie, C., 1979. A stratified water column environmental model for the type Kimmeridge Clay. Nature 277, 377–380.
Veizer, J., 1974. Chemical diagenesis of belemnite shells and possible consequences for paleotemperature determinations. Neues Jahrb. Geol. P-A. 147, 91–111.
Veizer, J., 1983. Chemical diagenesis of carbonates: theory and trace element technique. In: Arthur, M.A., Anderson, T.F., Kaplan, I.R., Veizer, J., Land, L.S. (Eds.), Stable Isotopes in Sedimentary Geology, SEPM Short Course No. 10, Dallas, pp. 3-1–3-100.
Veizer, J., Ala, D., Azmy, K., Bruckschen, P., Buhl, D., Bruhn, F., Carden, G.A.F., Diener, A., Ebneth, S., Godderis, Y., Jasper, T., Korte, C., Pawellek, F., Podlaha, O.G., Strauss, H., 1999. $^{87}Sr/^{86}Sr$, $\delta^{18}O$ and $\delta^{13}C$ Evolution of Phanerozoic seawater. Chem. Geol. 161, 59–88.
Vidier, J.P., Marchand, D., Bonnot, A., Fortwengler, D., 1993. The Callovian and Oxfordian of the Boulonnais area in northern France: new biostratigraphic data. Acta Geol. Pol. 43, 169–182.
Wefer, G., Berger, W.H., 1991. Isotope paleontology: growth and composition of extant calcareous species. Mar. Geol. 100, 207–248.
Westermann, G.E.G., 2000. Marine faunal realms of the Mesozoic: review and revision under the new guidelines for biogeographic classification and nomenclature. Palaeogeogr. Palaeoclimatol. Palaeoecol. 163, 49–68.
Wierzbowski, H., 2002. Detailed oxygen and carbon isotope stratigraphy of the Oxfordian in Central Poland. Int. J. Earth Sci. (Geol. Rundsch.) 91, 304–314.
Wierzbowski, H., 2004. Carbon and oxygen isotope composition of Oxfordian–Early Kimmeridgian belemnite rostra: palaeoenvironmental implications for Late Jurassic seas. Palaeogeogr. Palaeoclimatol. Palaeoecol. 203, 153–168.
Wierzbowski, H., Joachimski, M., 2007. Reconstruction of late Bajocian–Bathonian marine palaeoenvironments using carbon and oxygen isotope ratios of calcareous fossils from the Polish Jura Chain (central Poland). Palaeogeogr. Palaeoclimatol. Palaeoecol. 254, 523–540.
Wierzbowski, H., Dembicz, K., Praszkier, T., 2009. Oxygen and carbon isotope composition of Callovian–Lower Oxfordian (Middle–Upper Jurassic) belemnite rostra from central Poland: a record of a Late Callovian global sea-level rise? Palaeogeogr. Palaeoclimatol. Palaeoecol. 283, 182–194.
Ziegler, B., 1965. Boreale Einflüsse im Oberjura Westeuropas? Geol. Rundsch. 54, 250–261.
Ziegler, P.A., 1990. Geological Atlas of Western and Central Europe. Shell Internationale Petroleum Maatschappij B.V.